JGR Earth Surface

RESEARCH ARTICLE
10.1029/2022JF006772

Downstream Controls on Coastal Plain River Avulsions: A Global Study

Luca Colombera[1,2] **and Nigel P. Mountney**[2]

[1]Dipartimento di Scienze della Terra e dell'Ambiente, Università di Pavia, Pavia, Italy, [2]Fluvial, Eolian & Shallow-Marine Research Group, School of Earth and Environment, University of Leeds, Leeds, UK

Key Points:

- Holocene avulsion histories of 57 coastal plain river systems are analyzed
- Relationships between the intensity of wave and tides and river avulsion frequency are modest
- River avulsion frequency is not related to modern rates of absolute and relative sea-level change

Supporting Information:

Supporting Information may be found in the online version of this article.

Correspondence to:

L. Colombera,
luca.colombera@unipv.it

Citation:

Colombera, L., & Mountney, N. P. (2023). Downstream controls on coastal-plain river avulsions: A global study. *Journal of Geophysical Research: Earth Surface*, *128*, e2022JF006772. https://doi.org/10.1029/2022JF006772

Received 23 MAY 2022
Accepted 19 JAN 2023

Author Contributions:

Conceptualization: Luca Colombera
Data curation: Luca Colombera
Formal analysis: Luca Colombera
Funding acquisition: Luca Colombera, Nigel P. Mountney
Investigation: Luca Colombera
Methodology: Luca Colombera
Project Administration: Luca Colombera, Nigel P. Mountney
Resources: Luca Colombera
Writing – original draft: Luca Colombera
Writing – review & editing: Luca Colombera, Nigel P. Mountney

Abstract The avulsion frequency of coastal-plain rivers is primarily governed by the rate at which channels become superelevated over neighboring plains, which is itself controlled by multiple factors. Notably, the importance of wave and tidal processes, the rates of relative sea-level (RSL) change, and the bathymetry of the receiving basin are thought to affect channel morphodynamics and channel-mouth progradation, thereby controlling streambed aggradation and influencing the avulsion frequency and drainage density of coastal plains and deltas. This work tests the significance of these downstream factors on the avulsion histories of 57 Holocene lowland river systems. A quantitative analysis is performed of relationships between variables that quantify downstream controls and estimations of avulsion frequency, based on the number of avulsion events, active or abandoned channel paths, and delta lobes; measures of spatiotemporal avulsion "density" are also derived by normalizing these metrics by the size of study areas and the number of distinct drainage systems. Relationships between avulsion-frequency metrics and descriptors of process regime indicate that wave and tidal processes may stabilize coastal channel systems, but also that their influence may be modest. No consistent relationship is seen between avulsion-frequency proxies and the offshore bathymetric gradient, which in the studied examples does not scale with the rate of shoreline progradation. No evident trend exists between measures of avulsion frequency and estimated rates of either eustatic or RSL fluctuations. Overall, the considered variables do not leave a clear statistical signature in Holocene avulsion histories, suggesting that upstream or intrabasinal factors may represent more important controls.

Plain Language Summary Lowland rivers flowing near marine or lacustrine shorelines are affected by waves and tides, by relative variations in sea or lake level, and by the morphology of nearshore areas. These factors may affect the ability of coastal rivers to "avulse," that is, to establish new channel courses. This is expected because of how certain processes sculpt coastal landscapes: for example, waves may sweep sediment away from river mouths, tides can enhance sediment transfer along distributaries, and sea-level rise or seaward advance of the shoreline can drive vertical shifts in the elevation of riverbeds. These factors can variably determine the degree to which coastal river channels may become raised above neighboring coastal areas, a situation that makes them prone to diversion to new paths following levee breaching. The significance of these supposed controls is evaluated through statistical analyses of the number of (a) channel diversions, (b) historical channel paths, and (c) landforms or sediment bodies representing increments of delta growth (delta lobes), as recognized in the millennial to centennial histories of 57 fluvial systems. Waves and tides may play a modest role in stabilizing coastal rivers, but the studied factors appear to exert a limited control on river diversions overall.

1. Introduction

The drainage organization of coastal river systems, including deltas, is fundamentally determined by channel avulsions, that is, diversions of channels associated with the partial or complete abandonment of river reaches. In modern coastal environments, river avulsions constitute a form of flood hazard and dictate the spatiotemporal variability in sediment distribution to the coast and in related land-building processes (cf. Edmonds et al., 2009; Hoitink et al., 2020; Kleinhans et al., 2010). For sedimentary successions, river avulsions represent a key autogenic control on stratigraphic architectures, determining the geometry and stacking pattern of channel deposits and delta lobes (cf. Chamberlin & Hajek, 2015; Dalman et al., 2015; Flood & Hampson, 2014). Understanding the factors that control the frequency with which coastal rivers avulse is therefore important for interpreting the stratigraphic record, characterizing the geology of the subsurface, and predicting landscape change.

The factors that lead to river avulsions can be distinguished into (a) setup conditions that are created when the channel system reaches a metastable state, attained through the superelevation of the channel surface over the adjacent floodplain and establishment of gradient advantages away from the levees, and (b) triggers that cause levee breaks and initiate the new channel course, such as floods or tectonic events (Jones & Schumm, 1999; Slingerland & Smith, 2004). Although avulsion triggers may be dominantly determined by upstream or intrabasinal processes, a number of downstream controls are thought to affect avulsion setup conditions by regulating the rates at which channel ridges aggrade over coastal plains. Avulsion setup conditions can arise, for example, because of the concomitant aggradation of a channel as its longitudinal profile is extended while its mouth progrades basinward (Jones & Schumm, 1999). River-mouth progradation rates are determined by both upstream and downstream factors, namely by the rate of sediment supply (Aadland & Helland-Hansen, 2019; Colombera & Mountney, 2022) and existing accommodation. The latter factor is determined by the bathymetry of the seabed offshore of the coastal plain since it quantifies the sediment volume per unit shoreline length that is needed to achieve a certain amount of shoreline progradation over a given time interval, assuming no relative change in sea level (Muto & Steel, 1992). Indirect controls on river avulsions may also be operated by the process regime that governs coastal morphodynamics. Wave climate (wave height, period, direction) may represent one such forcing, since an increase in wave energy enhances the effect of longshore sediment transport on the redistribution of fluvial inputs in a way that should reduce rates of channel-mouth progradation and streambed aggradation, thereby hindering channel avulsion (Halbur, 2013; Ratliff et al., 2018; Swenson, 2005). Tides can also exert some influence: the flushing of tidally influenced fluvial channels by ebb-enhanced flows can facilitate sediment bypass, deepening and stabilizing distributary channels, and possibly reducing the frequency with which they avulse (Lentsch et al., 2018; Ragno et al., 2020; Rossi et al., 2016). Current understanding of the potential effects of relative sea-level (RSL) change on channel avulsion frequencies is rather more controversial. It is commonly thought that faster rates of RSL rise should promote more frequent river avulsions in relation to more rapid rates of channel-ridge aggradation (Chadwick et al., 2020; Jerolmack, 2009; Törnqvist, 1994), and that RSL falls may prevent channel relocations through valley incision (cf. Karamitopoulos et al., 2021). However, it is also recognized that sea-level falls may drive coastal-plain aggradation under favorable conditions of continental-shelf physiography (e.g., where the shelf gradient is gentler than the coastal plain gradient; Blum & Törnqvist, 2000), and that rates of base-level rise may control the degree to which streambed aggradation is distributed through the channel longitudinal profile, whereby a decrease in local aggradation rates associated with faster sea-level rise could in fact reduce avulsion frequency (Moran et al., 2017).

The aim of this work was to determine the importance of possible downstream controls on the frequency of coastal-plain river avulsions. This is achieved through (a) quantification of the Holocene avulsion histories of 57 coastal plains, as documented in the scientific literature, and (b) statistical analyses of relationships between proxies for avulsion frequency and quantities describing the nearshore process regime, sea-level change, and offshore bathymetry. This is done with consideration of how measures of avulsion frequency may be influenced by associated controls connected with the scale of the investigated river systems (Colombera & Mountney, 2022).

2. Data and Methods

2.1. Data Set

This study is based on literature-derived data on the evolution of 57 case studies of marine or lacustrine deltas and coastal plains (Figure 1), through timespans of the Holocene of variable duration (overall range: 0.033–10.8 kyr; Colombera & Mountney, 2022). All primary data sources are reported in Table S1 in Supporting Information S1. The studied river systems were characterized in terms of (a) paths of active or abandoned (paleo-) channels ("channel threads" hereafter), (b) occurrence of avulsion events, and/or (iii) location and extent of delta lobes. These features were originally determined based on historical records or maps, remote-sensing data (satellite images, aerial photos, LiDAR or InSAR elevation data), and field data on geomorphology and/or shallow subsurface stratigraphy (well and geophysical data). The avulsion histories of the case studies were inferred on the basis of radiometric dates, historical accounts, archeological evidence, and dated historical maps, satellite images, or aerial photos (Colombera & Mountney, 2022).

River avulsion frequencies were quantified by employing three alternative metrics (Colombera & Mountney, 2022): (a) the number of full or partial avulsion events that took place during the time window of data availability, (b) the number of channels leading to river mouths that were active during a time interval, but which may have already

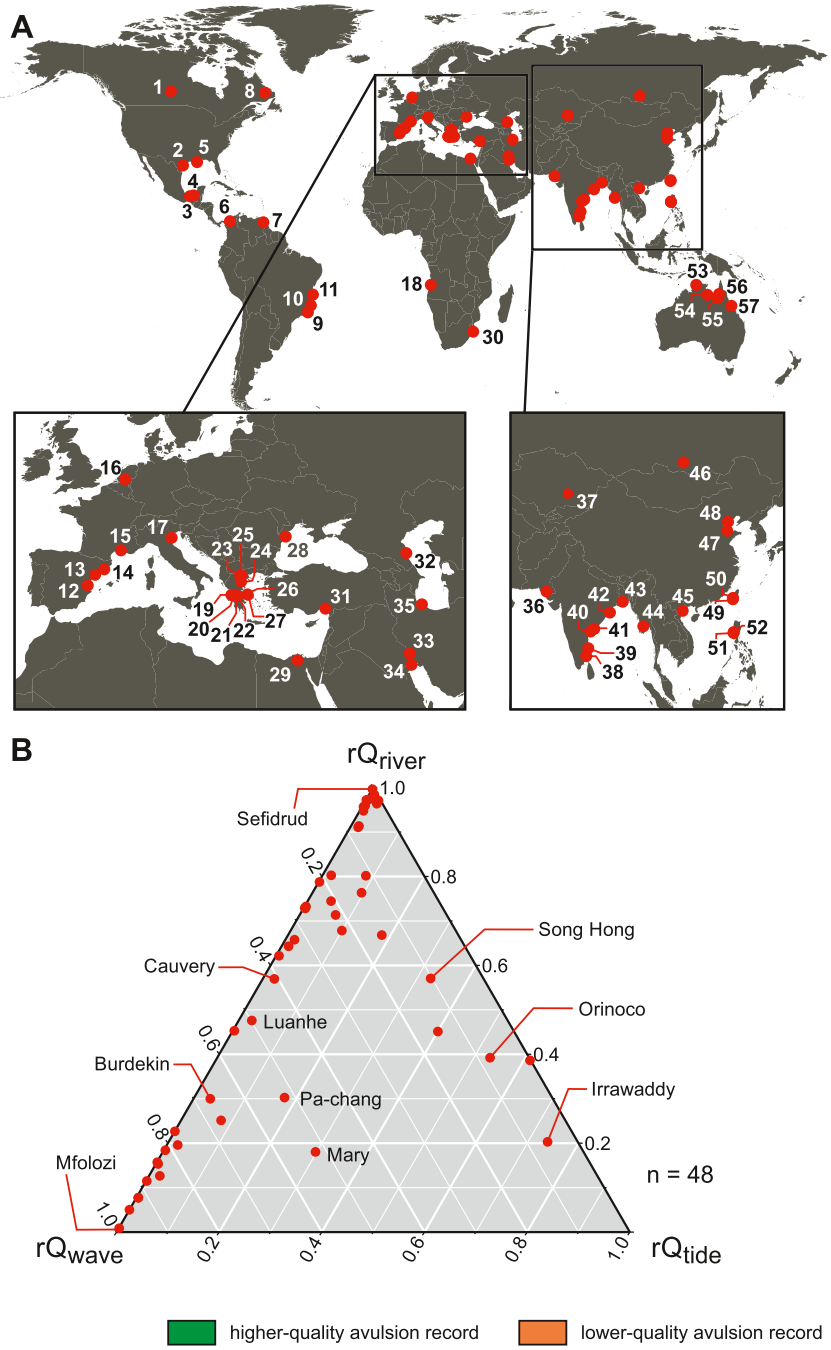

ID	river system	A	C	L
1	Saskatchewan			
2	San Antonio-Guadalupe			
3	Grijalva			
4	Usumacinta			
5	Mississippi			
6	Sinú			
7	Orinoco			
8	Goose			
9	Paraíba do Sul			
10	Doce			
11	Jequitinhonha			
12	Turia			
13	Ebro			
14	Llobregat			
15	Rhône			
16	Rhine-Meuse			
17	Po			
18	Catumbela			
19	Acheloos			
20	Evinos			
21	Mornos			
22	Selinous			
23	Aliakmon			
24	Pinios			
25	Axios			
26	Lilas			
27	Asopos			
28	Danube			
29	Nile			
30	Mfolozi			
31	Ceyhan-Seyhan			
32	Sulak			
33	Karkheh			
34	Shatt-al-Arab			
35	Sefidrud			
36	Indus			
37	Ili			
38	Cauvery			
39	Palar			
40	Krishna			
41	Godavari			
42	Mahanadi			
43	Bengal			
44	Irrawaddy			
45	Song Hong			
46	Selenga			
47	Huanghe			
48	Luanhe			
49	Tseng-wen			
50	Pa-chang			
51	Agno-Dagupan			
52	Bued-Patalan			
53	Mary			
54	McArthur			
55	Gilbert			
56	Mitchell			
57	Burdekin			

Figure 1. Summary of avulsion-history case studies. (a) Geographic distribution of the case studies of coastal-plain river systems considered in this work; numerical indices on the map refer to the identifiers ("ID") in the data summary on the right, where a classification of the completeness of their avulsion records is included. A: avulsion-event counts; C: channel-thread counts; L: delta-lobe counts. (b) Process regime of studied deltas expressed in terms of relative sediment flux (*rQ*) associated with river, wave and tidal processes, based on data from Nienhuis et al. (2020). Parts (a) and (b) are modified after Colombera and Mountney (2022).

been active at the beginning of the time window, and (c) the number of delta lobes that existed during the time window, where a delta lobe is defined as a sedimentary body made of genetically related delta-top, delta-front and prodelta deposits and associated with a state of river drainage established by avulsion. Alternative proxies for channel avulsion frequencies are computed as the number of avulsion events, channel threads, and delta lobes per unit time. Along with metrics defined as raw counts per unit time, additional measures of avulsion "density" in time and space are computed based on the normalization of each of these quantities with respect to the size of

the study area over which they are evaluated, that is, the planform extent of the delta plain or of the active part of coastal plain whose evolution was documented during the time of interest (Colombera & Mountney, 2022). For eight case studies documenting coastal plains traversed by rivers that joined intermittently during the Holocene, the same quantities are also normalized by the maximum number of river systems with distinct catchments that had independent drainage to the sea or lake at some point in time. Of the 57 case studies, 28 provide suitable data on avulsion events, 54 on channel threads, and 25 on delta lobes (Figure 1; Table S1 in Supporting Information S1); data sets that are unlikely to represent complete records of avulsion histories are flagged as being of "lower quality" to allow for separate analysis of "higher quality" avulsion records (Figure 1). A fuller account of the data set is provided by Colombera and Mountney (2022).

Data on potential downstream controls on river avulsion were derived from existing quantitative compilations and integrated where possible with data from ancillary literature sources. Data on the mean annual significant wave height and mean tidal range were obtained from the data set of Caldwell et al. (2019): wave heights are based on outputs of a 30-year hindcast by the wind wave model NOAA WAVEWATCH III (Chawla et al., 2013; Tolman, 2009); tidal ranges are based on computations on results of the global inverse model TOPEX/Poseidon (Egbert & Erofeeva, 2002). Data on the estimated sediment fluxes associated with rivers, waves and tides at the mouths of the studied rivers were taken from the global data set of Nienhuis et al. (2020). A measure of maximum potential wave-driven alongshore sediment flux (Q_w, hereafter) is also based on calculations on wave-energy data from WAVEWATCH III (Nienhuis et al., 2020). The tidal sediment-flux amplitude at river mouths (Q_t, hereafter) is instead based on quantifications of tidal amplitude and angular frequency, and channel aspect ratio and slope, as obtained from the TOPEX/Poseidon model, HydroSHEDS data (Lehner et al., 2008) and global SRTM topography (Nienhuis et al., 2020). Q_t is obtained by considering tidal flows as having the sediment concentration of river flows, and is proportional to the ratio between tidal water-discharge amplitude and mean annual river discharge (Nienhuis et al., 2020). Hence, in view of some scaling of avulsion metrics with river size (Colombera & Mountney, 2022), a normalization was applied in this study whereby Q_t is expressed relative to the rate of fluvial sediment supply, Q_r. Q_r is based on the WBMSed 2.0 distributed global-scale sediment flux model using the BQART approach (Cohen et al., 2013; Kettner & Syvitski, 2008). Q_r values that have been obtained for relatively pristine river conditions, to remove the effect of certain anthropogenic controls (Nienhuis et al., 2020), were used in this study. Values of Q_t normalized by Q_r effectively equate to tidal-to-fluvial water discharge ratios (a quantity termed "tidal dominance" by Nienhuis et al., 2018, 2020). Data on the bathymetries of the receiving basins offshore of river mouths and on rates of sea-level change were obtained from Caldwell et al. (2019). Gradients of the seabed within a 20-km radius of river mouths are derived from ETOPO1 bathymetric data (Amante & Eakins, 2009). Present-day rates of absolute sea-level change are based on AVISO satellite-altimetry data over the 1992–2018 period (Caldwell et al., 2019). Rates of RSL change due to glacioisostatic adjustment for the present day have been derived from the ICE-6G_C model, which is based on inputs specifying the history of ice-sheet loading and a five-layer viscosity profile (VM5a) of the Earth's interior (Peltier et al., 2015). Where available, data on measured rates of RSL rise based on observations over a 20-year period (1992–2013) are obtained from the ALTIGAPS database, which integrates GPS measurements, satellite radar altimetry and tide-gauge readings (Pfeffer & Allemand, 2016). Average shoreline progradation rates have been computed based on maps of dated paleoshorelines (Colombera & Mountney, 2022).

2.2. Limitations

This study is subject to limitations relating to both the avulsion metrics and the quantification of environmental controls (Colombera & Mountney, 2022). Counts of avulsion events may not be accurate due to the limited resolution of historical records, especially for older times. Avulsion histories do not include known artificial drainage changes, yet they may record undocumented artificial river diversions. Counts of channel threads may comprise distributary channels whose activation was not due to avulsion (e.g., unrecognized river-mouth bifurcations) and may not quantify avulsion events leading to reoccupation of abandoned reaches. The distinction of separate delta lobes may depend on the amount of lateral shift of a river mouth caused by avulsion. A more detailed account of limitations of the employed avulsion-frequency proxies is offered by Colombera and Mountney (2022).

The variables employed to quantify potential controls on river avulsions typically characterize modern-day conditions and as such their representativeness for millennial-scale avulsion histories may be very limited. For example, the wave climate can vary over short timescales (Reguero et al., 2019), and both wave and tidal processes

are affected by the physiography of the nearshore, which in some cases may have changed considerably through the Holocene. Modern rates of absolute sea-level fluctuations are generally considerably slower than the average Holocene sea-level rise (Lambeck et al., 2014). Employing these data allows assessment of geographic variations in sea-level change rather than variations through time, but present-day geographic variations are unlikely to be representative of geographic variability through the Holocene. Observed and modeled rates of RSL change are also based on the present day. Values based on the ICE-6G_C model ignore potential contributions by tectonics or sediment compaction. These estimations are also subject to significant uncertainty relating to the model inputs (Melini & Spada, 2019); discrepancies with measured rates have been documented (Engelhart et al., 2011; Roy & Peltier, 2018). Observed present-day rates of RSL change are only available for 15 case studies. Rates of shoreline progradation have been extracted over different timescales, but these rates are time-dependent over the considered spatial scales (see Colombera & Mountney, 2022). The length scale over which the bathymetric gradient is defined (20-km radius; Caldwell et al., 2019) is comparable with the average shoreline progradation distance of the studied coastal plains (17.0 km); however, there exists significant variability in the length of shoreline progradation across the studied examples (range 1.0–81.3 km), and the original bathymetric profiles over which the studied coasts prograded likely exhibited gradients that differed from the present-day ones.

The existence of gaps in the data set, owing to the fact that some of the considered variables could not be constrained in several cases, limits the types of analyses that can be undertaken with it. Although multivariate analyses are desired in a study of this type, they cannot be performed over all the chosen case studies with the available data. Statistical analyses may also be affected by a bias in the data because documented avulsion histories may preferentially exist for rivers that are highly avulsive; the global representativeness of the selected case studies could not be established. Measures of correlation might be systematically weaker due to attenuation bias or error in some of the considered variables (Muchinsky, 1996).

2.3. Statistical Analyses

The sign and magnitude of relationships between metrics of avulsion frequency and the variables describing potential downstream controls on river avulsion have been assessed by Pearson correlation coefficients of the variables or of their logarithmic transformations; Spearman's correlation coefficients have also been employed for graphical representation of monotonic relationships that may not be linear. The statistical significance of correlations is quantified by two-tailed p values. These p values have not been corrected for multiple comparisons; therefore, special care must be taken in considering possible false positives (Armstrong, 2014). All analyses are performed over the entire data pool as well as separately on data from examples classed as having "higher quality" avulsion histories (Figure 1). Analyses have been undertaken in R 4.2.1 (R Core Team, 2021).

3. Results

Both raw and normalized avulsion metrics are used in our analyses. Colombera and Mountney (2022) showed that, in the data set, the spatiotemporal density of avulsion events, as quantified by normalized avulsion metrics, is not independent of study area size, that is, the inferred frequency of avulsion events is not directly proportional to the size of the area over which they occur. This may be due to (a) variations in the resolution with scale, (b) to spatial non-stationarity in channel avulsion (e.g., because avulsions occurring preferentially at delta-apex nodes may operate according to a similar rhythm regardless of delta scale), or (iii) to variations in the importance of avulsion controls with the size of the river system, to which study areas tend to be scaled (Colombera & Mountney, 2022). In analyses involving normalized avulsion rates, it must be borne in mind that covariance exists between the study-area size (e.g., extent of delta plain) on which normalization is made, river-system size, and scale-dependent variables (e.g., water discharge, sediment load).

Data on relationships between avulsion metrics and possible downstream controls are presented in Figures 2–5; the results of correlation analyses are presented in Tables 1–4 and in Figure 6.

No significant correlation is observed between mean annual significant wave heights and any of the avulsion metrics (Figures 2 and 6, Table 1). Similarly, significant relationships between wave-driven alongshore sediment flux (Q_w) and avulsion proxies based on avulsion-event, channel-thread or delta-lobe counts are not seen; however, Q_w demonstrates statistically significant (for $\alpha = 0.05$) negative relationships with normalized values of all three avulsion metrics, albeit of moderate magnitude (Figures 2 and 6, Table 1). As expected, some

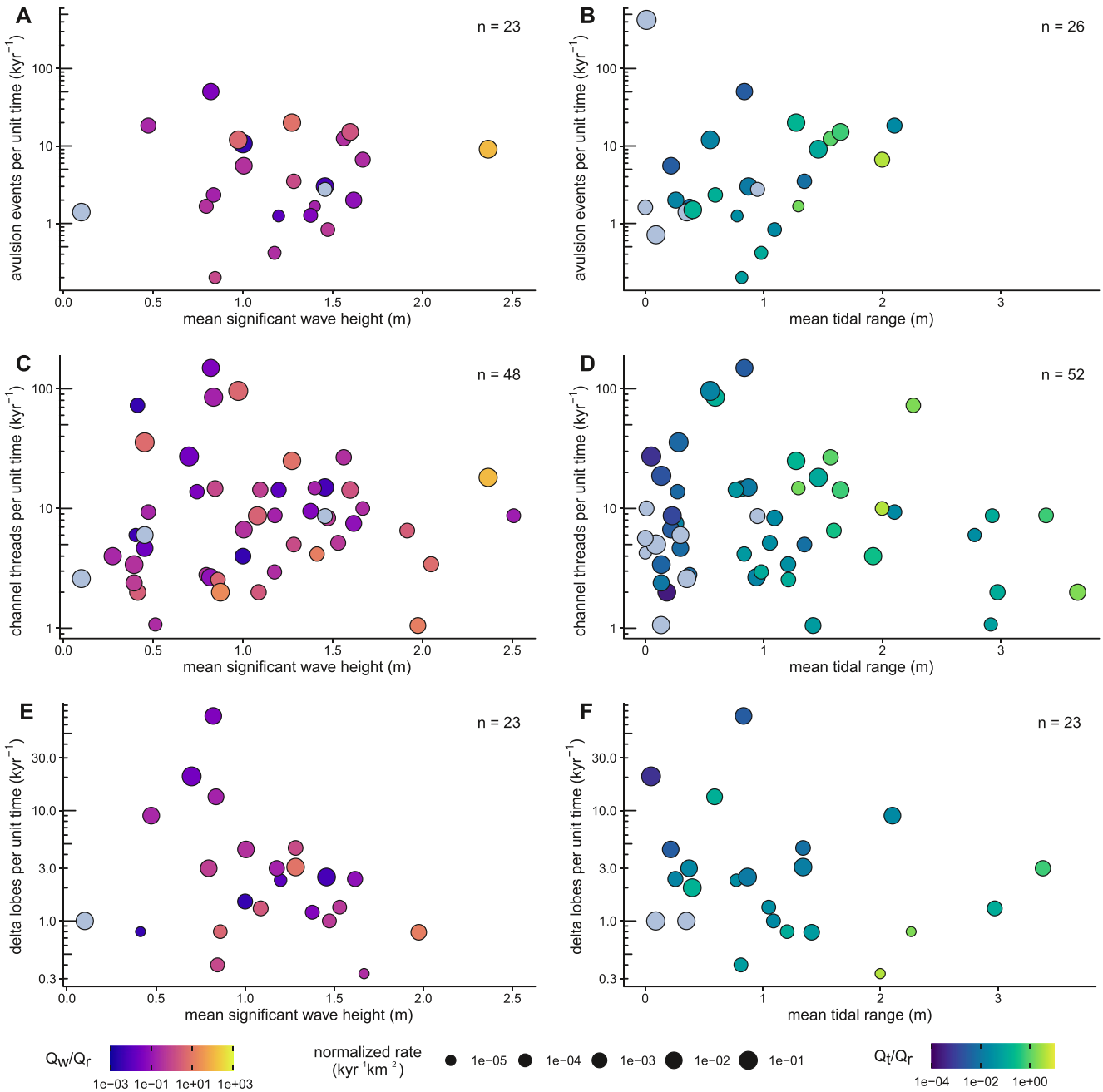

Figure 2. Scatterplots of mean significant wave height and mean tidal range against avulsion-frequency metrics based on the number of avulsion events (a, b), channel threads (c, d), and delta lobes (e, f). The size of the spots indicates values of normalized avulsion metrics. Spot colors indicate values of ratios between longshore (Q_w) or tidal (Q_t) sediment flux and fluvial sediment flux (Q_r).

positive correlation exists between mean wave height and Q_w (for log-transformed Q_w values: Pearson $R = 0.543$, $p < 0.001$, $N = 46$; Figure 6). No significant correlation is seen between shoreline progradation rates (i.e., rates of progradation averaged over the length of coast, rather than solely at river mouths) and either mean wave height (for log-transformed values: Pearson $R = 0.162$, $p = 0.376$, $N = 32$; Figure 6) or wave-driven longshore sediment flux, Q_w (for log-transformed values: Pearson $R = 0.150$, $p = 0.405$, $N = 33$; Figure 6). Instead, a positive correlation exists between progradation rates and fluvial sediment flux (Q_r) (for log-transformed values: $R = 0.667$, $p < 0.001$, $N = 33$; Figure 6; cf. Colombera & Mountney, 2022).

No consistent relationship exists between the mean tidal range and avulsion metrics that are not normalized by the size of the study area (Figure 2, Table 2). Negative relationships are instead observed between the mean

tidal range and all normalized avulsion metrics, but the correlation is weak and not significant for normalized rates based on avulsion-event counts (Figures 2 and 6, Table 2). Similar results are observed in the relationships between avulsion metrics and the Q_t/Q_r ratio, which corresponds to the tidal-to-fluvial water-discharge ratio, that is, the "tidal dominance" of Nienhuis et al. (2020) (Figures 2 and 6, Table 2). The expected positive relationship between the tidal range and the Q_t/Q_r ratio is seen (for log-transformed Q_t/Q_r ratios: Pearson $R = 0.667$, $p < 0.001$, $N = 46$; Figure 6). Both Q_t and Q_r are directly correlated with the size of the study areas, in relation to covariance between study-area size, river-system size, and sediment loads (Colombera & Mountney, 2022); the magnitude of correlation is similar for the two variables (for Q_r: $R = 0.803$, $p < 0.001$, $N = 48$; for Q_t: $R = 0.833$, $p < 0.001$, $N = 48$; correlations of log-transformed values). However, the Q_t/Q_r ratio demonstrated some positive correlation with the size of the study area (for log-transformed values: $R = 0.466$, $p < 0.001$, $N = 48$).

Only one of the considered examples is associated with a currently ongoing absolute fall in the base level: its avulsion metrics fall within the range of examples associated with a base-level rise. The analysis is hence focused on the role of the rate of eustatic base-level rise (Figures 3 and 6). No significant correlation is observed between present-day rates of absolute sea-level change and the avulsion-frequency proxies, with the exception of modest negative relationships with normalized avulsion-event and channel-thread densities (Figures 3 and 6, Table 3). No evident difference in the magnitude of avulsion proxies is seen across groups of examples characterized by current relative base-level rise or fall driven by glacioisostatic adjustment; however, the former group consists of only five river systems, and all but two of the systems that are presently under conditions of RSL fall are characterized by limited rates of change (less than 0.4 mm/yr; Figure 3). If observations of RSL change are considered rather than the modeled glacioisostatic components, most examples are associated with conditions of relative rise. Significant relationships between observed rates of RSL rise and the avulsion metrics are not seen (Figure 4, Table 3).

No consistent relationship is observed between the seabed gradient offshore of river mouths and the different avulsion-frequency metrics (Figures 5 and 6, Table 4). This is in accord with the observation of a lack of correlation between rates of shoreline progradation and the offshore gradient (for log-transformed values: Pearson $R = -0.036$, $p = 0.843$, $N = 33$; cf. Figure 6).

In view of the outcomes of these analyses regarding the poor predictive power of the considered variables, a regression model that would account for downstream controls on avulsion frequency is not proposed.

4. Discussion

The considered avulsion-frequency proxies vary over orders of magnitude, indicating that different coastal-plain river systems can differ widely with respect to avulsion dynamics. The current work allows the evaluation of the degree to which external controls acting downstream of the river systems may determine this variability (cf. Colombera & Mountney, 2022).

Among these factors, the process regime of marine or lacustrine coastal systems is commonly advocated as a potential control on channel avulsion. For example, numerical models demonstrate the potential impact of wave influence on inter-avulsion periods (Ratliff et al., 2018; Swenson, 2005), whereby avulsion setup conditions are affected by longshore sediment transport through its controls on river-mouth progradation, basinward channel lengthening, and associated streambed aggradation (Jones & Schumm, 1999). This notion is supported by the analysis of channel networks across classes of deltas that reflect inferred wave influence (Halbur, 2013). Wave climate also controls the accretion of sets of beach ridges on wave-dominated deltas, whose topographic relief may hinder avulsions by confining channels (Syvitski & Saito, 2007). In the current study, these types of control by the wave climate may be expressed in the negative relationships between values of present-day longshore sediment flux (Q_w), accounting for wave energy (Nienhuis et al., 2020), and normalized avulsion rates, which quantify the spatiotemporal density of avulsion events through Holocene timespans. Yet, correlations between Q_w and these avulsion metrics are modest, and no significant correlation is seen between values of mean significant wave height and avulsion proxies, which might instead have been expected (cf. Ratliff et al., 2018). Moreover, neither mean wave height nor Q_w is inversely correlated with rates of shoreline progradation; said rates are based on coast-wide averages, however, and therefore they do not necessarily reflect the rates at which individual river mouths may have prograded. In addition, the results may be partially related to other forms of control using wave processes on channel networks. For instance, they may reflect the way by which waves inhibit the formation

of mouth bars (Jerolmack & Swenson, 2007), and hence the establishment of channel bifurcations that may contribute to the number of paleochannels preserved on coastal plains (Edmonds & Slingerland, 2007). Overall, nonetheless, these findings suggest that the influence of wave energy on river avulsions is modest, and that upstream controls may dominate over longshore redistribution in determining rates of river-mouth progradation and channel avulsions (cf. Colombera & Mountney, 2022).

The potential influence of tides on channel morphodynamics has also been investigated by the outputs of numerical models (Ragno et al., 2020; Rossi et al., 2016) as well as by physical experiments (Lentsch et al., 2018): these earlier studies indicate that the erosive action of tidal currents in distributary channels may enhance their stability and reduce their avulsion frequency. In addition, observations on modern systems (Hoitink et al., 2017) suggest that tide-influenced lowland river reaches—whose length scale is a function of the importance of tides—may also be less susceptible to flooding relative to upstream areas; this may be reflected in the frequency with which avulsions are triggered in these contexts. These controls may be expressed in the observed negative relationships between normalized avulsion-frequency metrics and both the mean tidal range and values of Q_t/Q_r ratio (equivalent to a tidal-to-fluvial discharge ratio Nienhuis et al., 2020). These results might confirm that the influence of tides on river mobility is not limited to tide-dominated systems, but that it rather plays a role in micro- to meso-tidal settings too. However, the Q_t/Q_r ratio tends to covary with the size of the study areas relative to which the avulsion metrics are normalized, and the normalized metrics themselves tend to decrease with increasing study-area size (Colombera & Mountney, 2022); this may partly explain the results. Furthermore, no significant relationship is seen for metrics based on avulsion-event counts nor for avulsion-frequency proxies that are not normalized. Also, the results may reflect other ways in which tides may control the drainage organization of lowland river systems: for example, tides—like waves—may reduce the tendency of channels to bifurcate by preventing mouth-bar growth (Rossi et al., 2016), and this may again have influenced the number of channel threads present. In any case, the magnitude of correlation between normalized avulsion metrics and measures of tidal range and sediment flux is modest overall; any effect of tides on river avulsion is likely to be limited.

The importance of the rate and direction of base-level change on inter-avulsion periods is broadly recognized, although the manner in which their influence may be expressed is disputed. A widely held assumption is that river avulsion frequency should scale directly with the rate of base-level rise: a river system tied to a rising base level is expected to maintain equilibrium by streambed aggradation, which would ultimately cause superelevation of channel ridges over neighboring floodbasins or interdistributary bays (Jerolmack, 2009; Törnqvist, 1994). Temporal variations in the inferred avulsion frequency of Holocene deltas have been interpreted in these terms (e.g., Aslan & Autin, 1999; Stouthamer et al., 2011), and this view is supported by results of numerical models (e.g., Chadwick & Lamb, 2021; Chadwick et al., 2020; Jerolmack, 2009). Yet, results of a 1D morphodynamic model suggest instead that more rapid rates of base-level rise could determine streamwise changes in streambed aggradation, associated with a decrease in maximum aggradation relative to the channel depth, and that this could cause an increase—not a decrease—in inter-avulsion periods (Moran et al., 2017). Numerical models also demonstrate that if channel progradation is sufficiently rapid, river avulsions are not sensitive to the rates of sea-level rise, and that this may be a characteristic condition of river-dominated systems with rapidly advancing coasts (Ratliff et al., 2018). Elucidating the potential role of RSL changes on channel avulsions carries implications for sequence stratigraphic models, which tend to link stratigraphic variations in channel body geometries and stacking patterns to base-level states via their relationships with sediment accommodation space (e.g., Wright & Marriott, 1993) because changes in avulsion periods can also produce similar trends (cf. Bryant et al., 1995; Colombera et al., 2015). In the coastal-plain systems of the current study, significant negative relationships are seen between rates of absolute sea-level rise for the last three decades and normalized counts of avulsion events and channel threads; these correlations are of modest magnitude, however, and non-normalized avulsion metrics are not negatively correlated with sea-level rise. The results may appear to clash with the intuition that a faster rate of base-level rise should drive more frequent avulsions, on the assumption that geographic variations in present-day rates of absolute sea-level change are representative of spatial changes that were persistent throughout the Holocene. However, this assumption is likely unrealistic since geographic variations in sea-level change over decadal timescales, associated chiefly with ocean thermal expansion and changes in salinity, are of transient nature (Meyssignac et al., 2012). Geographic variations in present-day rates of RSL change are more likely to have persisted over much of the studied avulsion histories and are more directly relevant as controls on deltaic morphodynamics. Thus, more meaningful indications of the limited importance of the direction and speed of RSL fluctuations on coastal-plain avulsions can be drawn from (a) the lack of any apparent difference in avulsion

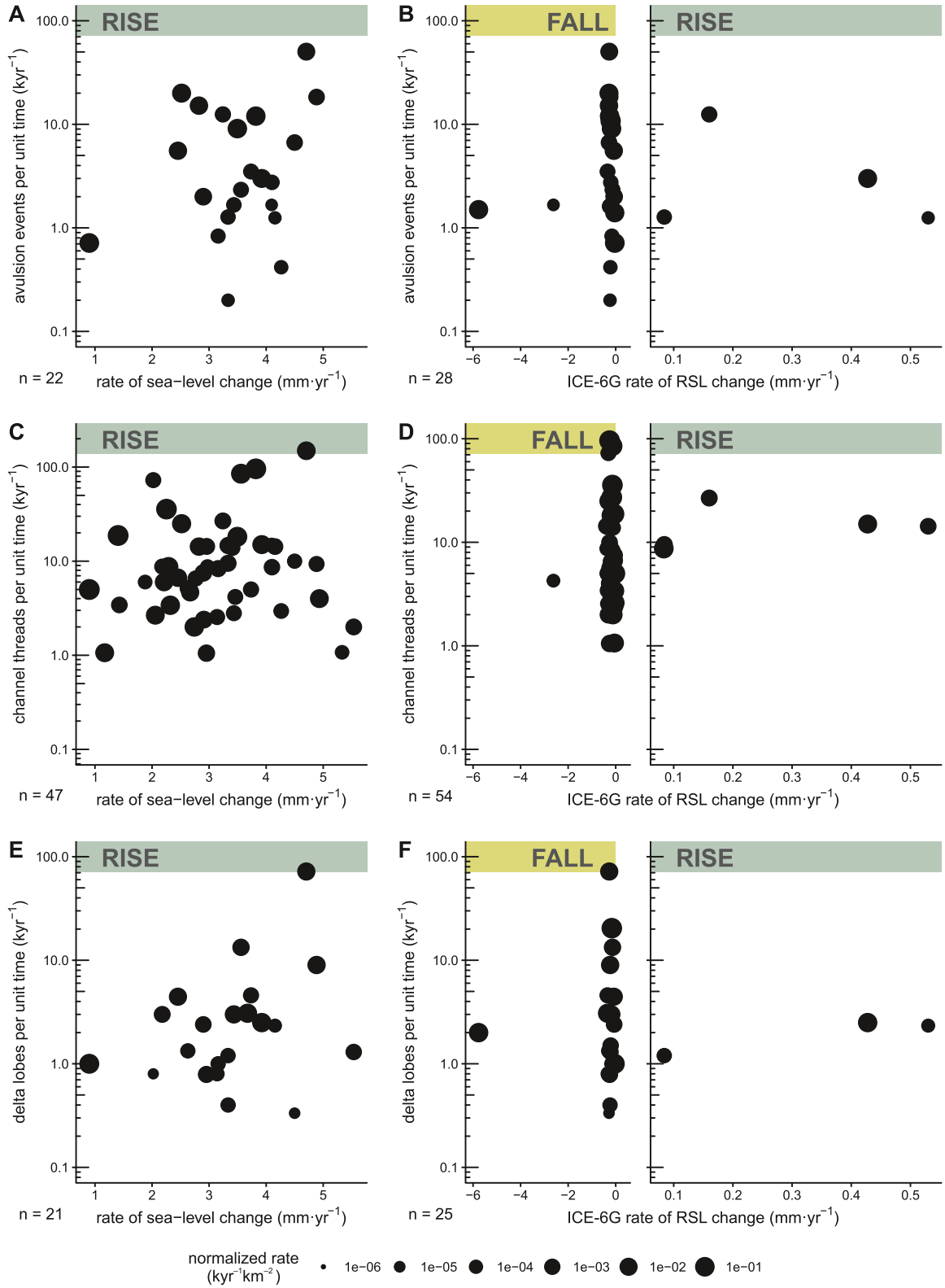

Figure 3. Scatterplots of rate of eustatic sea-level change (left-hand side) and glacioisostatic relative sea-level (RSL) change (right-hand side) against avulsion-frequency metrics based on numbers of avulsion events (a, b), channel threads (c, d) and delta lobes (e, f). The size of the spots indicates values of normalized avulsion metrics.

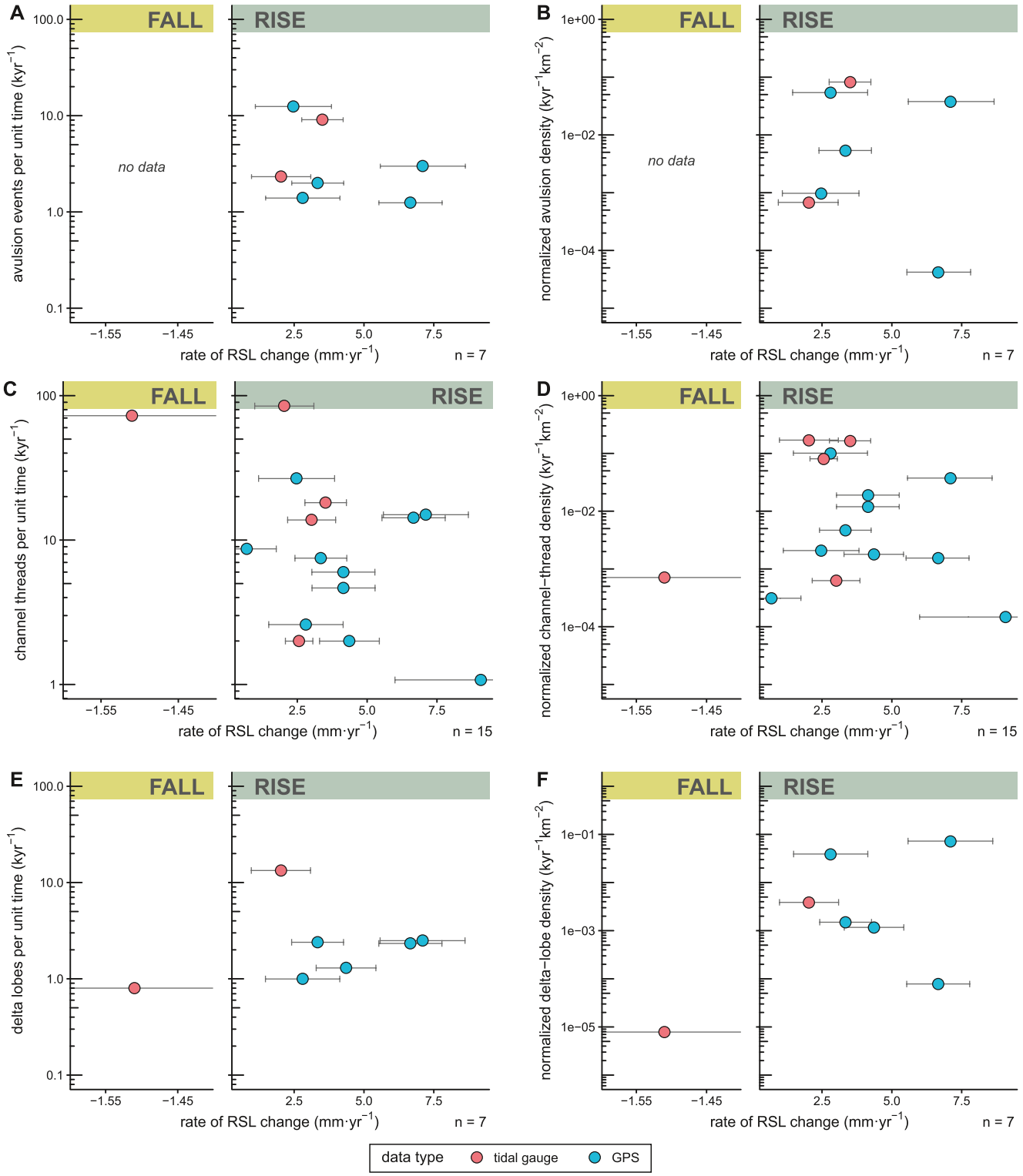

Figure 4. Scatterplots of rates of measured relative sea-level (RSL) change against avulsion-frequency metrics based on numbers of avulsion events (a, b), channel threads (c, d) and delta lobes (e, f); raw (left-hand side) and normalized (right-hand side) avulsion metrics are separately presented. Spots are color coded by the type of observation on which the RSL change is determined. Error bars represent two standard deviations in RSL data.

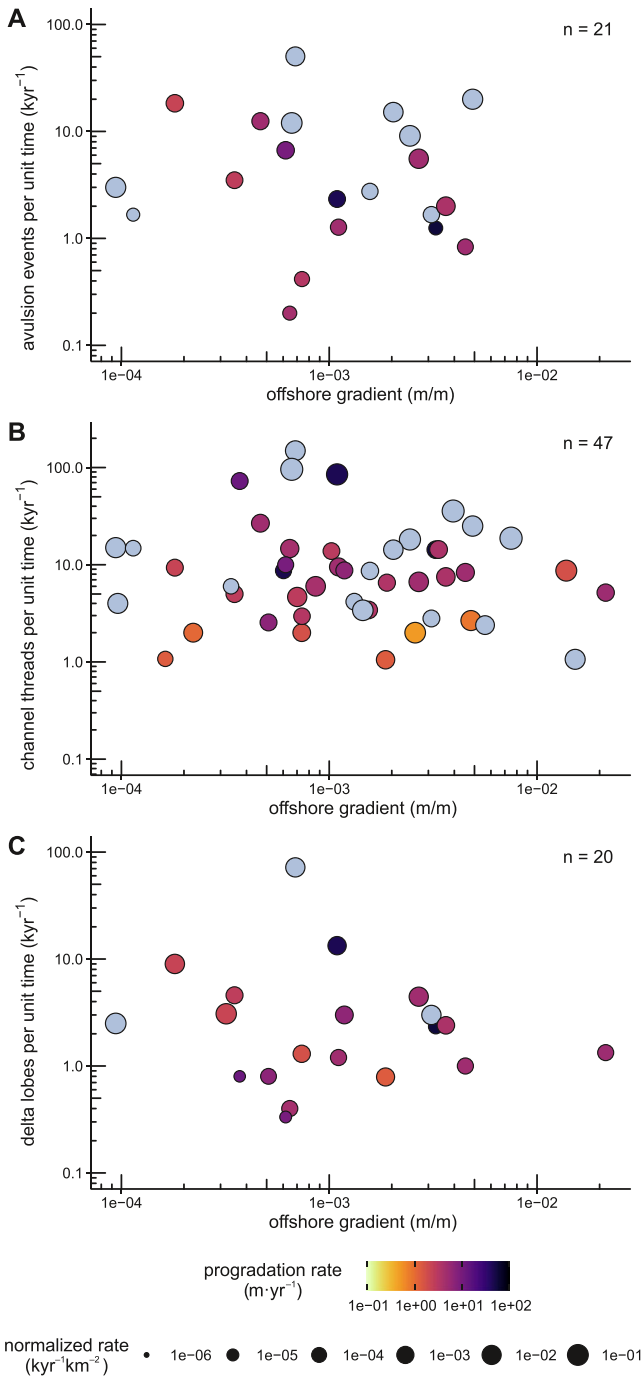

Figure 5. Scatterplots of offshore gradient against avulsion-frequency metrics based on the number of avulsion events (a, b), channel threads (c, d) and delta lobes (e, f). The size of the spots indicates values of normalized avulsion metrics. Spot colors indicate values of mean shoreline progradation rate (see Colombera & Mountney, 2022).

metrics across case studies associated with negative, near-zero, and positive rates of glacioisostatic RSL change and (b) the lack of significant relationships between the avulsion-frequency metrics and available measurements of present-day RSL change. However, glacioisostatic rates only represent valid estimates over centennial timescales, and measured rates of RSL changes are determined over decadal timescales; the current analysis can be improved by employing direct constraints of RSL variations over the same timescales of avulsion records, where available.

Additional insight can be obtained from a complementary analysis of the dependency of avulsion-frequency metrics on the length of time over which they have been determined: since the avulsion histories are usually tied to the present day, any such dependency may reflect temporal variations in avulsion frequency through the Holocene (Colombera & Mountney, 2022), which could be considered in light of the progressive deceleration of global sea-level rise through the Holocene (Lambeck et al., 2014). For the studied marginal-marine systems, negative correlations are seen between the avulsion-frequency metrics and their associated timespans, which may reflect a progressive increase in avulsion frequency through the Holocene, in parallel with the global decrease in the rate of sea-level rise (Colombera & Mountney, 2022). These results should be taken with care, however, since this time-dependency of inter-avulsion periods may merely reflect variations in the resolution of avulsion records, which likely becomes coarser as the time window expands to older times (Colombera & Mountney, 2022).

The idea that RSL falls should prevent channel relocations through valley incision is intuitive and supported by existing numerical models (cf. Harriset al., 2020; Karamitopoulos et al., 2021); however, river avulsions are documented in deltaic systems experiencing base-level falls (Blair & McPherson, 1994; Lane et al., 2017; Nijhuis et al., 2015). Depending on the physiography of the receiving basin (and particularly the relative gradient of coastal plain vs. continental shelf), the coastal plain may aggrade—rather than become incised—through forced regressions (Blum & Törnqvist, 2000; Slingerland & Smith, 2004). The development of channel superelevation during RSL falls has been documented in modern systems, where avulsion frequency may have increased in response to a fall in base level (cf. Lane et al., 2017; Nijhuis et al., 2015). This complexity of responses may explain the observation that avulsion-frequency metrics for systems associated with absolute or RSL falls do not differ significantly from those that are respectively associated with absolute or relative rises.

In summary, the rate and direction of eustatic or RSL changes do not seem to have affected the avulsion dynamics of the studied coastal-plain systems in a manner that is consistent across all quantifications of avulsion frequency and the entire data pool; this suggests that the importance of sea level as a control on river avulsion may vary depending on depositional setting and may be subordinate to that of other factors.

The bathymetry of the seabed offshore of coastal plains may be expected to demonstrate relationships with quantifications of the progradation of river mouths and of channel avulsions. In part, this might be expected because the bathymetry of the seabed may be scaled with the size of the study areas relative to which the avulsion metrics are normalized. However, any such relationship may additionally arise due to the influence of marine accommodation on shoreline progradation rates and/or due to covariance of the nearshore bathymetry with factors that may also act to control the dynamics of coastal channel networks. For example, the seabed gradient is a function of the type of sediment being supplied, which is itself related to the rate of sediment supply, and hence to river-system size (Milliman &

Table 1
Pearson Correlation Coefficients and Associated p Values Quantifying Relationships Between Log-Transformed Avulsion-Frequency Metrics (A: Avulsion-Event Counts; C: Channel-Thread Counts; L: Delta-Lobe Counts) and Both Mean Significant Wave Height and Estimated Longshore Sediment Flux (Q_w)

	Normalization	Mean wave height	Q_w
A	None	$R = 0.089$, $p = 0.685$, $N = 23$	$R = -0.087$, $p = 0.701$, $N = 22$
		($R = 0.052$, $p = 0.859$, $N = 14$)	($R = 0.036$, $p = 0.907$, $N = 13$)
	By area and river number	$R = 0.004$, $p = 0.986$, $N = 23$	$R = -0.479$, $p = 0.024$, $N = 22$
		($R = 0.028$, $p = 0.924$, $N = 14$)	($R = -0.311$, $p = 0.301$, $N = 13$)
C	None	$R = 0.058$, $p = 0.696$, $N = 48$	$R = 0.062$, $p = 0.680$, $N = 46$
		($R = 0.060$, $p = 0.698$, $N = 44$)	($R < 0.001$, $p > 0.999$, $N = 42$)
	By area and river number	$R = -0.232$, $p = 0.113$, $N = 48$	$R = -0.406$, $p = 0.005$, $N = 46$
		($R = -0.218$, $p = 0.155$, $N = 44$)	($R = -0.442$, $p = 0.003$, $N = 42$)
L	None	$R = -0.280$, $p = 0.196$, $N = 23$	$R = -0.276$, $p = 0.202$, $N = 23$
		($R = -0.336$, $p = 0.221$, $N = 15$)	($R = -0.096$, $p = 0.733$, $N = 15$)
	By area and river number	$R = -0.238$, $p = 0.273$, $N = 23$	$R = -0.573$, $p = 0.004$, $N = 23$
		($R = -0.372$, $p = 0.172$, $N = 15$)	($R = -0.642$, $p = 0.010$, $N = 15$)

Note. Statistics in brackets refer to higher-quality data sets only (Figure 1).

Farnsworth, 2011). Shelf gradients can also control progradation rates indirectly, by affecting the process regime that drives sediment dispersal in the nearshore, for example, through the dissipation of wave energy (Swift & Thorne, 1991). More fundamentally, however, the bathymetric gradient, as the rate of offshore increase in water depth, determines the amount of accommodation available near the coast (cf. Colombera & Mountney, 2020; Heward, 1981): for steeper seabeds, a higher rate of sediment supply per unit shoreline length is required to sustain a given rate or progradation. Notwithstanding, in the studied examples, no significant relationship is seen between the offshore gradient and either the avulsion-frequency metrics or the related shoreline progradation rates. For data on avulsion histories associated with longer (millennial) time windows, a lack of correlation may be determined by differences between present-day gradients and earlier Holocene bathymetries: the considered bathymetric slope may not be a suitable proxy for sediment accommodation. However, the results

Table 2
Pearson Correlation Coefficients and Associated p Values Quantifying Relationships Between Log-Transformed Avulsion-Frequency Metrics (A: Avulsion-Event Counts; C: Channel-Thread Counts; L: Delta-Lobe Counts) and Both Mean Tidal Range and the Ratio Between Tidal and Fluvial Sediment Fluxes (Q_t/Q_r)

	Normalization	Mean tidal range	Q_t/Q_r
A	None	$R = 0.195$, $p = 0.341$, $N = 26$	$R = 0.115$, $p = 0.610$, $N = 22$
		($R = 0.087$, $p = 0.739$, $N = 17$)	($R = 0.206$, $p = 0.499$, $N = 13$)
	By area and river number	$R = -0.172$, $p = 0.402$, $N = 26$	$R = -0.161$, $p = 0.475$, $N = 22$
		($R = -0.129$, $p = 0.621$, $N = 17$)	($R = -0.134$, $p = 0.662$, $N = 13$)
C	None	$R = -0.102$, $p = 0.473$, $N = 52$	$R = 0.105$, $p = 0.487$, $N = 46$
		($R = -0.100$, $p = 0.494$, $N = 49$)	($R = 0.114$, $p = 0.473$, $N = 42$)
	By area and river number	$R = -0.449$, $p = 0.001$, $N = 52$	$R = -0.281$, $p = 0.059$, $N = 46$
		($R = -0.437$, $p = 0.002$, $N = 49$)	($R = -0.232$, $p = 0.139$, $N = 42$)
L	None	$R = -0.203$, $p = 0.354$, $N = 23$	$R = -0.402$, $p = 0.057$, $N = 23$
		($R = -0.157$, $p = 0.576$, $N = 15$)	($R = -0.018$, $p = 0.950$, $N = 15$)
	By area and river number	$R = -0.470$, $p = 0.024$, $N = 23$	$R = -0.560$, $p = 0.005$, $N = 23$
		($R = -0.253$, $p = 0.363$, $N = 15$)	($R = 0.028$, $p = 0.922$, $N = 15$)

Note. Statistics in brackets refer to higher-quality data sets only (Figure 1).

Table 3
Pearson Correlation Coefficients and Associated p Values Quantifying Relationships Between Log-Transformed Avulsion-Frequency Metrics (A: Avulsion-Event Counts; C: Channel-Thread Counts; L: Delta-Lobe Counts) and Rates of Absolute and Relative Sea-Level Rise

	Normalization	Rate of eustatic sea-level rise	Rate of relative sea-level rise
A	None	$R = 0.221$, $p = 0.322$, $N = 22$	$R = -0.333$, $p = 0.465$, $N = 7$
		($R = 0.017$, $p = 0.956$, $N = 13$)	Dis-attenuated $R = -0.409$
	By area and river number	$R = -0.434$, $p = 0.043$, $N = 22$	$R = 0.019$, $p = 0.967$, $N = 7$
		($R = -0.293$, $p = 0.331$, $N = 13$)	Dis-attenuated $R = 0.024$
C	None	$R = 0.069$, $p = 0.643$, $N = 47$	$R = -0.116$, $p = 0.695$, $N = 14$
		($R = 0.030$, $p = 0.849$, $N = 43$)	Dis-attenuated $R = -0.144$
	By area and river number	$R = -0.365$, $p = 0.012$, $N = 47$	$R = 0.137$, $p = 0.203$, $N = 14$
		($R = -0.418$, $p = 0.005$, $N = 43$)	Dis-attenuated $R = 0.171$
L	None	$R = 0.303$, $p = 0.182$, $N = 21$	$R = -0.476$, $p = 0.340$, $N = 6$
		($R = 0.271$, $p = 0.348$, $N = 14$)	Dis-attenuated $R = -0.581$
	By area and river number	$R = -0.071$, $p = 0.759$, $N = 21$	$R = 0.401$, $p = 0.310$, $N = 6$
		($R = 0.066$, $p = 0.822$, $N = 14$)	Dis-attenuated $R = 0.431$

Note. Statistics in brackets refer to higher-quality data sets only (Figure 1). Dis-attenuated correlation coefficients (Muchinsky, 1996) are presented for relationships with values of rates of relative sea-level rise, to account for errors in estimated rates.

can be interpreted to indicate that shoreline and river-mouth progradation rates are more readily controlled by sediment-supply rates than by basin accommodation (Colombera & Mountney, 2022), in accord with current understanding (Aadland & Helland-Hansen, 2019).

Collectively, the findings of this study indicate that the influence of downstream controls on the avulsion frequency of coastal-plain rivers may be more limited than often implied. This may reflect the overriding role of upstream or intrabasinal controls as well as the possibility that the inherent self-organization of coastal-plain river systems is not particularly sensitive to allogenic controls (cf. Colombera & Mountney, 2022). However, additional analysis of the current data set with explicit consideration of all possible controlling factors is still required. Also, the precise timing of avulsion is known for parts of the temporal evolutions of some of the considered case-study river systems; these may lend themselves to additional analyses of response times to external forcings.

Table 4
Pearson Correlation Coefficients and Associated p Values Quantifying Relationships Between Log-Transformed Avulsion-Frequency Metrics (A: Avulsion-Event Counts; C: Channel-Thread Counts; L: Delta-Lobe Counts) and the Seabed Gradient Offshore of the Studied River Mouths

	Normalization	Offshore gradient
A	None	$R = -0.046$, $p = 0.843$, $N = 21$
		($R = -0.089$, $p = 0.772$, $N = 13$)
	By area and river number	$R = 0.157$, $p = 0.495$, $N = 21$
		($R = 0.101$, $p = 0.742$, $N = 13$)
C	None	$R = -0.153$, $p = 0.305$, $N = 47$
		($R = 0.260$, $p = 0.092$, $N = 43$)
	By area and river number	$R = 0.244$, $p = 0.099$, $N = 47$
		($R = -0.126$, $p = 0.421$, $N = 43$)
L	None	$R = -0.112$, $p = 0.638$, $N = 20$
		($R = -0.271$, $p = 0.348$, $N = 14$)
	By area and river number	$R = -0.141$, $p = 0.554$, $N = 20$
		($R = -0.403$, $p = 0.153$, $N = 14$)

Note. Statistics in brackets refer to higher-quality data sets only (Figure 1).

5. Conclusions

Quantitative analyses of the avulsion histories of 57 Holocene coastal river systems, undertaken employing metrics based on the number of avulsion events, channel threads and delta lobes, have allowed the statistical evaluation of the possible role of downstream factors as controls on channel avulsion. These factors include measures of the contribution of wave and tidal processes in nearshore environments, of rates and direction of absolute and relative base-level changes and of the physiography of the seabed offshore of the river mouths. These factors are all expected to affect channel-ridge aggradation—a necessary condition for river avulsion—either directly or through their effect on river-mouth progradation.

The hypotheses that avulsion frequency should scale directly with the rate of base-level rise, or inversely with the offshore gradient, do not find support in the presented data set. The view that wave and tidal processes can act to stabilize lowland channel networks is instead supported by some of the results. In general, however, the relationships between the considered

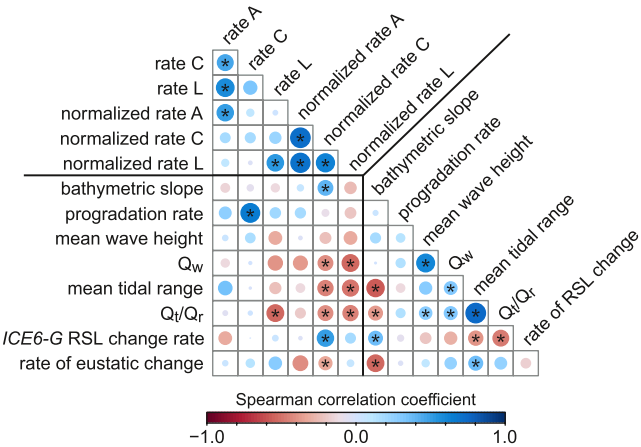

Figure 6. Heatmap of Spearman correlation coefficients quantifying relationships between avulsion-frequency metrics and characteristics of the river systems. Asterisks denote significant correlations ($p < 0.05$). A: avulsion events per unit time; C: channel threads per unit time; L: delta lobes per unit time; RSL: relative sea level. Normalized rates are based on normalization by area and river number. Only modeled rates of relative sea-level change due to glacioisostasy are included in these results.

avulsion-frequency metrics and the supposed controlling factors are not strong, and neither are they expressed consistently across the different proxies. The influence of downstream controls on the avulsion frequency of coastal rivers does not leave an evident signature on avulsion statistics.

It is recognized, nonetheless, that this study is hampered by significant data limitations, notably related to the completeness of avulsion records and to the limited degree to which attributes quantifying present-day environmental controls may be relevant to the mid to late Holocene. It is recommended that such a study be replicated with a more refined data set when this becomes available.

A key implication of this study is that river avulsions are not particularly affected by downstream controls, perhaps because intrabasinal or upstream controls (e.g., levee stability, discharge variability) are dominant, or because allogenic factors have limited influence on the studied autogenic dynamics. Yet, specific investigation of the role of all possible controls on coastal channel avulsion is still needed.

Data Availability Statement

The data used in this article are stored in the Research Data Repository of the University of Leeds (Colombera, 2022), and can be accessed at https://doi.org/10.5518/1148.

Acknowledgments
We thank the sponsors of the Fluvial, Eolian & Shallow-Marine Research Group for financial support to this research (AkerBP, Areva [now Orano], BHP, Cairn India [Vedanta], Chevron, CNOOC International, ConocoPhillips, Equinor, Murphy Oil, Occidental, Saudi Aramco, Shell, Tullow Oil, Woodside, and YPF). Eric Barefoot, Gary Weissmann and an anonymous referee are thanked for their constructive reviews, which have improved the article. Open Access Funding provided by Università degli Studi di Pavia within the CRUI-CARE Agreement.

References

Aadland, T., & Helland-Hansen, W. (2019). Progradation rates measured at modern river outlets: A first-order constraint on the pace of deltaic deposition. *Journal of Geophysical Research: Earth Surface*, *124*(2), 347–364. https://doi.org/10.1029/2018jf004750

Amante, C., & Eakins, B. W. (2009). *ETOPO1 arc-minute global relief model: Procedures, data sources and analysis*. NOAA Technical Memorandum NESDIS NGDC-24, National Geophysical Data Center, NOAA.

Armstrong, R. A. (2014). When to use the Bonferroni correction. *Ophthalmic and Physiological Optics*, *34*(5), 502–508. https://doi.org/10.1111/opo.12131

Aslan, A., & Autin, W. J. (1999). Evolution of the Holocene Mississippi River floodplain, Ferriday, Louisiana; insights on the origin of fine-grained floodplains. *Journal of Sedimentary Research*, *69*(4), 800–815. https://doi.org/10.2110/jsr.69.800

Blair, T. C., & McPherson, J. G. (1994). Historical adjustments by Walker River to lake-level fall over a tectonically tilted half-graben floor, Walker Lake Basin, Nevada. *Sedimentary Geology*, *92*(1–2), 7–16. https://doi.org/10.1016/0037-0738(94)00058-1

Blum, M. D., & Törnqvist, T. E. (2000). Fluvial responses to climate and sea-level change: A review and look forward. *Sedimentology*, *47*(s1), 2–48. https://doi.org/10.1046/j.1365-3091.2000.00008.x

Bryant, M., Falk, P., & Paola, C. (1995). Experimental study of avulsion frequency and rate of deposition. *Geology*, *23*(4), 365–368. https://doi.org/10.1130/0091-7613(1995)023<0365:esoafa>2.3.co;2

Caldwell, R. L., Edmonds, D. A., Baumgardner, S., Paola, C., Roy, S., & Nienhuis, J. H. (2019). A global delta dataset and the environmental variables that predict delta formation on marine coastlines. *Earth Surface Dynamics*, *7*(3), 773–787. https://doi.org/10.5194/esurf-7-773-2019

Chadwick, A. J., & Lamb, M. P. (2021). Climate-change controls on river delta avulsion location and frequency. *Journal of Geophysical Research: Earth Surface*, *126*(6), e2020JF005950. https://doi.org/10.1029/2020JF005950

Chadwick, A. J., Lamb, M. P., & Ganti, V. (2020). Accelerated river avulsion frequency on lowland deltas due to sea-level rise. *Proceedings of the National Academy of Sciences*, *117*(30), 17584–17590. https://doi.org/10.1073/pnas.1912351117

Chamberlin, E. P., & Hajek, E. A. (2015). Interpreting paleo-avulsion dynamics from multistory sand bodies. *Journal of Sedimentary Research*, *85*(2), 82–94. https://doi.org/10.2110/jsr.2015.09

Chawla, A., Spindler, D. M., & Tolman, H. L. (2013). Validation of a thirty year wave hindcast using the Climate Forecast System Reanalysis winds. *Ocean Modelling*, *70*, 189–206. https://doi.org/10.1016/j.ocemod.2012.07.005

Cohen, S., Kettner, A. J., Syvitski, J. P., & Fekete, B. M. (2013). WBMsed, a distributed global-scale riverine sediment flux model: Model description and validation. *Computers & Geosciences*, *53*, 80–93. https://doi.org/10.1016/j.cageo.2011.08.011

Colombera, L. (2022). FRG-SMRG Coastal rivers avulsion dataset [Dataset]. University of Leeds. https://doi.org/10.5518/1148

Colombera, L., & Mountney, N. P. (2020). Accommodation and sediment-supply controls on clastic parasequences: A meta-analysis. *Sedimentology*, *67*(4), 1667–1709. https://doi.org/10.1111/sed.12728

Colombera, L., & Mountney, N. P. (2022). Scale dependency in quantifications of the avulsion frequency of coastal rivers. *Earth-Science Reviews*, *230*, 104043. https://doi.org/10.1016/j.earscirev.2022.104043

Colombera, L., Mountney, N. P., & McCaffrey, W. D. (2015). A meta-study of relationships between fluvial channel-body stacking pattern and aggradation rate: Implications for sequence stratigraphy. *Geology*, *43*(4), 283–286. https://doi.org/10.1130/g36385.1

Dalman, R., Weltje, G. J., & Karamitopoulos, P. (2015). High-resolution sequence stratigraphy of fluvio–deltaic systems: Prospects of system-wide chronostratigraphic correlation. *Earth and Planetary Science Letters*, *412*, 10–17. https://doi.org/10.1016/j.epsl.2014.12.030

Edmonds, D. A., Hoyal, D. C., Sheets, B. A., & Slingerland, R. L. (2009). Predicting delta avulsions: Implications for coastal wetland restoration. *Geology*, *37*(8), 759–762. https://doi.org/10.1130/g25743a.1

Edmonds, D. A., & Slingerland, R. L. (2007). Mechanics of river mouth bar formation: Implications for the morphodynamics of delta distributary networks. *Journal of Geophysical Research*, *112*(F2), F02034. https://doi.org/10.1029/2006JF000574

Egbert, G. D., & Erofeeva, S. Y. (2002). Efficient inverse modeling of barotropic ocean tides. *Journal of Atmospheric and Oceanic Technology*, *19*(2), 183–204. https://doi.org/10.1175/1520-0426(2002)019<0183:eimobo>2.0.co;2

Engelhart, S. E., Peltier, W. R., & Horton, B. P. (2011). Holocene relative sea-level changes and glacial isostatic adjustment of the US Atlantic coast. *Geology*, *39*(8), 751–754. https://doi.org/10.1130/g31857.1

Flood, Y. S., & Hampson, G. J. (2014). Facies and architectural analysis to interpret avulsion style and variability: Upper Cretaceous Blackhawk formation, Wasatch Plateau, central Utah, USA. *Journal of Sedimentary Research*, *84*(9), 743–762. https://doi.org/10.2110/jsr.2014.59

Halbur, J. (2013). *Frequency and spatial distribution of avulsion nodes on river deltas as a function of wave energy* M.Sc. Thesis. University of Minnesota.

Harris, A. D., Covault, J. A., Baumgardner, S., Sun, T., & Granjeon, D. (2020). Numerical modeling of icehouse and greenhouse sea-level changes on a continental margin: Sea-level modulation of deltaic avulsion processes. *Marine and Petroleum Geology*, *111*, 807–814. https://doi.org/10.1016/j.marpetgeo.2019.08.055

Heward, A. P. (1981). A review of wave-dominated clastic shoreline deposits. *Earth-Science Reviews*, *17*(3), 223–276. https://doi.org/10.1016/0012-8252(81)90022-2

Hoitink, A. J. F., Nittrouer, J. A., Passalacqua, P., Shaw, J. B., Langendoen, E. J., Huismans, Y., & van Maren, D. S. (2020). Resilience of river deltas in the Anthropocene. *Journal of Geophysical Research: Earth Surface*, *125*(3), e2019JF005201. https://doi.org/10.1029/2019JF005201

Hoitink, A. J. F., Wang, Z. B., Vermeulen, B., Huismans, Y., & Kästner, K. (2017). Tidal controls on river delta morphology. *Nature Geoscience*, *10*(9), 637–645. https://doi.org/10.1038/ngeo3000

Jerolmack, D. J. (2009). Conceptual framework for assessing the response of delta channel networks to Holocene sea level rise. *Quaternary Science Reviews*, *28*(17–18), 1786–1800. https://doi.org/10.1016/j.quascirev.2009.02.015

Jerolmack, D. J., & Swenson, J. B. (2007). Scaling relationships and evolution of distributary networks on wave-influenced deltas. *Geophysical Research Letters*, *34*(23), L23402. https://doi.org/10.1029/2007GL031823

Jones, L. S., & Schumm, S. A. (1999). Causes of avulsion: An overview. In N. D. Smith & J. Rogers (Eds.), *Fluvial sedimentology VI* (pp. 169–178). Wiley & Sons.

Karamitopoulos, P., Weltje, G. J., & Dalman, R. A. (2021). Large-scale connectivity of fluvio-deltaic stratigraphy: Inferences from simulated accommodation-to-supply cycles and automated extraction of chronosomes. *Basin Research*, *33*(1), 382–402. https://doi.org/10.1111/bre.12471

Kettner, A. J., & Syvitski, J. P. (2008). HydroTrend v. 3.0: A climate-driven hydrological transport model that simulates discharge and sediment load leaving a river system. *Computers & Geosciences*, *34*(10), 1170–1183. https://doi.org/10.1016/j.cageo.2008.02.008

Kleinhans, M. G., Weerts, H. J., & Cohen, K. M. (2010). Avulsion in action: Reconstruction and modelling sedimentation pace and upstream flood water levels following a medieval tidal-river diversion catastrophe (Biesbosch, The Netherlands, 1421–1750 AD). *Geomorphology*, *118*(1–2), 65–79. https://doi.org/10.1016/j.geomorph.2009.12.009

Lambeck, K., Rouby, H., Purcell, A., Sun, Y., & Sambridge, M. (2014). Sea level and global ice volumes from the Last Glacial Maximum to the Holocene. *Proceedings of the National Academy of Sciences*, *111*(43), 15296–15303. https://doi.org/10.1073/pnas.1411762111

Lane, T. I., Nanson, R. A., Vakarelov, B. K., Ainsworth, R. B., & Dashtgard, S. E. (2017). Evolution and architectural styles of a forced-regressive Holocene delta and megafan, Mitchell River, Gulf of Carpentaria, Australia. In G. J. Hampson, A. D. Reynolds, B. Kostic, & M. R. Wells (Eds.), *Sedimentology of paralic reservoirs: Recent advances* (Vol. 444, pp. 305–334). Geological Society, London, Special Publications.

Lehner, B., Verdin, K., & Jarvis, A. (2008). New global hydrography derived from spaceborne elevation data. *Eos, Transactions American Geophysical Union*, *89*(10), 93–94. https://doi.org/10.1029/2008eo100001

Lentsch, N., Finotello, A., & Paola, C. (2018). Reduction of deltaic channel mobility by tidal action under rising relative sea level. *Geology*, *46*(7), 599–602. https://doi.org/10.1130/g45087.1

Melini, D., & Spada, G. (2019). Some remarks on glacial isostatic adjustment modelling uncertainties. *Geophysical Journal International*, *218*(1), 401–413. https://doi.org/10.1093/gji/ggz158

Meyssignac, B., Becker, M., Llovel, W., & Cazenave, A. (2012). An assessment of two-dimensional past sea level reconstructions over 1950–2009 based on tide-gauge data and different input sea level grids. *Surveys in Geophysics*, *33*(5), 945–972. https://doi.org/10.1007/s10712-011-9171-x

Milliman, J. D., & Farnsworth, K. L. (2011). *River discharge to the coastal ocean: A global synthesis*. Cambridge University Press.

Moran, K. E., Nittrouer, J. A., Perillo, M. M., Lorenzo-Trueba, J., & Anderson, J. B. (2017). Morphodynamic modeling of fluvial channel fill and avulsion time scales during early Holocene transgression, as substantiated by the incised valley stratigraphy of the Trinity River, Texas. *Journal of Geophysical Research: Earth Surface*, *122*(1), 215–234. https://doi.org/10.1002/2015JF003778

Muchinsky, P. M. (1996). The correction for attenuation. *Educational and Psychological Measurement*, *56*(1), 63–75. https://doi.org/10.1177/0013164496056001004

Muto, T., & Steel, R. J. (1992). Retreat of the front in a prograding delta. *Geology*, *20*(11), 967–970. https://doi.org/10.1130/0091-7613(1992)020<0967:rotfia>2.3.co;2

Nienhuis, J. H., Ashton, A. D., Edmonds, D. A., Hoitink, A. J. F., Kettner, A. J., Rowland, J. C., & Törnqvist, T. E. (2020). Global-scale human impact on delta morphology has led to net land area gain. *Nature*, *577*(7791), 514–518. https://doi.org/10.1038/s41586-019-1905-9

Nienhuis, J. H., Hoitink, A. J. F., & Törnqvist, T. E. (2018). Future change to tide-influenced deltas. *Geophysical Research Letters*, *45*(8), 3499–3507. https://doi.org/10.1029/2018GL077638

Nijhuis, A. G., Edmonds, D. A., Caldwell, R. L., Cederberg, J. A., Slingerland, R. L., Best, J. L., et al. (2015). Fluvio-deltaic avulsions during relative sea-level fall. *Geology*, *43*(8), 719–722. https://doi.org/10.1130/g36788.1

Peltier, W. R., Argus, D. F., & Drummond, R. (2015). Space geodesy constrains ice age terminal deglaciation: The global ICE-6G_C (VM5a) model. *Journal of Geophysical Research: Solid Earth*, *120*(1), 450–487. https://doi.org/10.1002/2014JB011176

Pfeffer, J., & Allemand, P. (2016). The key role of vertical land motions in coastal sea level variations: A global synthesis of multisatellite altimetry, tide gauge data and GPS measurements. *Earth and Planetary Science Letters*, *439*, 39–47. https://doi.org/10.1016/j.epsl.2016.01.027

Ragno, N., Tambroni, N., & Bolla Pittaluga, M. (2020). Effect of small tidal fluctuations on the stability and equilibrium configurations of bifurcations. *Journal of Geophysical Research: Earth Surface*, *125*(8), e2020JF005584. https://doi.org/10.1029/2020JF005584

Ratliff, K. M., Hutton, E. H., & Murray, A. B. (2018). Exploring wave and sea-level rise effects on delta morphodynamics with a coupled river-ocean model. *Journal of Geophysical Research: Earth Surface*, *123*(11), 2887–2900. https://doi.org/10.1029/2018JF004757

R Core Team. (2021). *R: A language and environment for statistical computing*. R Foundation for Statistical Computing. Retrieved from https://www.R-project.org/

Reguero, B. G., Losada, I. J., & Méndez, F. J. (2019). A recent increase in global wave power as a consequence of oceanic warming. *Nature Communications*, *10*(1), 1–14. https://doi.org/10.1038/s41467-018-08066-0

Rossi, V. M., Kim, W., Leva López, J., Edmonds, D., Geleynse, N., Olariu, C., et al. (2016). Impact of tidal currents on delta-channel deepening, stratigraphic architecture, and sediment bypass beyond the shoreline. *Geology*, *44*(11), 927–930. https://doi.org/10.1130/g38334.1

Roy, K., & Peltier, W. R. (2018). Relative sea level in the Western Mediterranean basin: A regional test of the ICE-7G_NA (VM7) model and a constraint on late Holocene Antarctic deglaciation. *Quaternary Science Reviews*, *183*, 76–87. https://doi.org/10.1016/j.quascirev.2017.12.021

Slingerland, R., & Smith, N. D. (2004). River avulsions and their deposits. *Annual Review of Earth and Planetary Sciences*, *32*(1), 257–285. https://doi.org/10.1146/annurev.earth.32.101802.120201

Stouthamer, E., Cohen, K. M., & Gouw, M. J. (2011). Avulsion and its implications for fluvial deltaic architecture: Insights from the Holocene Rhine-Meuse Delta. In S. K. Davidson, S. Leleu, & C. P. North (Eds.), *From River to rock record: The preservation of fluvial sediments and their Subsequent interpretation* (Vol. 97, pp. 215–231). SEPM Special Publication.

Swenson, J. B. (2005). Relative importance of fluvial input and wave energy in controlling the timescale for distributary-channel avulsion. *Geophysical Research Letters*, *32*(23), GL024758. https://doi.org/10.1029/2005GL024758

Swift, D. J. P., & Thorne, J. A. (1991). Sedimentation on continental margins, I: A general model for shelf sedimentation. In D. J. P. Swift, G. F. Oertel, R. W. Tillman, & J. A. Thorne (Eds.), *Shelf sand and sandstone bodies–geometry, facies, and sequence stratigraphy* (Vol. 14, pp. 3–31). International Association of Sedimentologists, Special Publication.

Syvitski, J. P., & Saito, Y. (2007). Morphodynamics of deltas under the influence of humans. *Global and Planetary Change*, *57*(3–4), 261–282. https://doi.org/10.1016/j.gloplacha.2006.12.001

Tolman, H. L. (2009). *User manual and system documentation of WAVEWATCH III version 4.18* (p. 282). U.S. Department of Commerce, National Oceanic and Atmospheric Administration National Weather Service, National Centers for Environmental Prediction.

Törnqvist, T. E. (1994). Middle and late Holocene avulsion history of the River Rhine (Rhine-Meuse delta, Netherlands). *Geology*, *22*(8), 711–714. https://doi.org/10.1130/0091-7613(1994)022<0711:malhah>2.3.co;2

Wright, V. P., & Marriott, S. B. (1993). The sequence stratigraphy of fluvial depositional systems: The role of floodplain sediment storage. *Sedimentary Geology*, *86*(3–4), 203–210. https://doi.org/10.1016/0037-0738(93)90022-w

References From the Supporting Information

Abdrasilov, S. A., & Tulebaeva, K. A. (1994). Dynamics of the Ili delta with consideration of fluctuations of the level of Lake Balkhash. *Hydrotechnical Construction*, *28*(8), 421–426. https://doi.org/10.1007/bf01487447

Ainsworth, R. B., Vakarelov, B. K., Eide, C. H., Howell, J. A., & Bourget, J. (2019). Linking the high-resolution architecture of modern and ancient wave-dominated deltas: Processes, products, and forcing factors. *Journal of Sedimentary Research*, *89*(2), 168–185. https://doi.org/10.2110/jsr.2019.7

Akter, J., Sarker, M. H., Popescu, I., & Roelvink, D. (2016). Evolution of the Bengal Delta and its prevailing processes. *Journal of Coastal Research*, *32*(5), 1212–1226. https://doi.org/10.2112/jcoastres-d-14-00232.1

Al-Hamad, S. S., Albadran, B. N., & Pournelle, J. R. (2017). Geological history of Shatt Al-Arab river, South of Iraq. *International Journal of Science and Research*, *6*(1), 2029–2039.

Allison, M. A., Khan, S. R., Goodbred, S. L., Jr., & Kuehl, S. A. (2003). Stratigraphic evolution of the late Holocene Ganges–Brahmaputra lower delta plain. *Sedimentary Geology*, *155*(3–4), 317–342. https://doi.org/10.1016/s0037-0738(02)00185-9

Aslan, A., White, W. A., Warne, A. G., & Guevara, E. H. (2003). Holocene evolution of the western Orinoco Delta, Venezuela. *The Geological Society of America Bulletin*, *115*(4), 479–498. https://doi.org/10.1130/0016-7606(2003)115<0479:heotwo>2.0.co;2

Ataol, M. (2015). A crevasse splay induced avulsion on the Ceyhan delta. *The Journal of International Social Research*, 8(41), 675–681. https://doi.org/10.17719/jisr.20154115048

Berendsen, H. J. A., & Stouthamer, E. (2002). Paleogeographic evolution and avulsion history of the Holocene Rhine-Meuse delta, The Netherlands. *Netherlands Journal of Geosciences*, *81*(1), 97–112. https://doi.org/10.1017/s0016774600020606

Bhattacharya, J. P., Miall, A. D., Ferron, C., Gabriel, J., Randazzo, N., Kynaston, D., et al. (2019). Time-stratigraphy in point sourced river deltas: Application to sediment budgets, shelf construction, and paleo-storm records. *Earth-Science Reviews*, *199*, 102985. https://doi.org/10.1016/j.earscirev.2019.102985

Bondesan, M., Favero, V., & Viñals, M. J. (1995). New evidence on the evolution of the Po-delta coastal plain during the Holocene. *Quaternary International*, *29*, 105–110. https://doi.org/10.1016/1040-6182(95)00012-8

Chamberlain, E. L., Törnqvist, T. E., Shen, Z., Mauz, B., & Wallinga, J. (2018). Anatomy of Mississippi Delta growth and its implications for coastal restoration. *Science Advances*, *4*(4), eaar4740. https://doi.org/10.1126/sciadv.aar4740

Chang, J. C., & Chen, H. L. (2001). Geomorphological changes on coastal plain in southwestern Taiwan. *Western Pacific Earth Sciences*, *1*(1), 107–114.

Chen, D., Li, X., Saito, Y., Liu, J. P., Duan, Y., & Zhang, L. (2020). Recent evolution of the Irrawaddy (Ayeyarwady) delta and the impacts of anthropogenic activities: A review and remote sensing survey. *Geomorphology*, *365*, 107231. https://doi.org/10.1016/j.geomorph.2020.107231

Cheng, L., Xu, Q., Guo, H., Li, M., Yang, N., Liu, J., et al. (2020). The late Holocene stratum and evolution in the Luanhe River Delta. *Quaternary Sciences*, *40*(3), 751–763. https://doi.org/10.27355/d.cnki.gtjsy.2020.000012

Correggiari, A., Cattaneo, A., & Trincardi, F. (2005a). Depositional patterns in the late Holocene Po delta system. In L. Giosan & J. P. Bhattacharya (Eds.), *River deltas—concepts, models, and examples* (Vol. 83, pp. 13–30). SEPM Special Publication.

Correggiari, A., Cattaneo, A., & Trincardi, F. (2005b). The modern Po delta system: Lobe switching and asymmetric prodelta growth. *Marine Geology*, *222*, 49–74. https://doi.org/10.1016/j.margeo.2005.06.039

Cuong, T. Q. (2009). *Soil properties, topography and quaternary substratum in the edge of the Red River delta, Vietnam* Doctoral dissertation. University of Natural Resources and Applied Life Sciences.

Da Rocha, T. B. (2013). *A planície costeira meridional do complexo deltáico do rio Paraíba do Sul (RJ): Arquitetura deposicional e evolução da paisagem durante o Quaternário Tardio* Doctoral dissertation. Universidade Federal do Rio de Janeiro.

Dash, C., Jaiswal, M. K., Pati, P., Patel, N. K., Singh, A. K., & Shah, R. A. (2020). Fluvial response to Late Quaternary sea level changes along the Mahanadi delta, east coast of India. *Quaternary International*, *553*, 60–72. https://doi.org/10.1016/j.quaint.2020.07.033

Deom, J. M., Sala, R., & Laudisoit, A. (2019). The Ili river delta: Holocene hydrogeological evolution and human colonization. In L. E. Yang, H. R. Bork, X. Fang, & S. Mischke (Eds.), *Socio-environmental dynamics along the historical silk road* (pp. 67–94). Springer.

Dinis, P. A., Huvi, J., & Callapez, P. M. (2018). The Catumbela delta (SW Angola). Processes determining a history of changing asymmetry. *Journal of African Earth Sciences*, *145*, 68–79. https://doi.org/10.1016/j.jafrearsci.2018.05.001

Dominguez, J. M. L., Bittencourt, A. C. S. P., & Martin, L. (1981). Esquema evolutivo da sedimentaçao quaternaria nas feiçoes deltaicas dos rios Sao Francisco (SE/AL), Jequitinhonha (BA), Doce (ES) e Paraiba do Sul (RJ). *Revista Brasileira de Geociencias*, *11*(4), 227–237. https://doi.org/10.25249/0375-7536.1981227237

Donaldson, A. C., Martin, R. H., & Kanes, W. H. (1970). Holocene Guadalupe delta of Texas gulf coast. In J. P. Morgan (Ed.), *Deltaic sedimentation modern and ancient* (Vol. 15, pp. 107–137). SEPM Special Publication.

Dong, T. Y. (2020). *Dynamics of delta building across different scales as informed by the Selenga River Delta, Russia* Doctoral dissertation. Rice University.

El Bastawesy, M., Gebremichael, E., Sultan, M., Attwa, M., & Sahour, H. (2020). Tracing Holocene channels and landforms of the Nile Delta through integration of early elevation, geophysical, and sediment core data. *The Holocene*, *30*(8), 1129–1141. https://doi.org/10.1177/0959683620913928

Erol, O. (2003). Geomorphological evolution of the Ceyhan river delta: Eastern Mediterranean coast of Turkey. *Aegean Geographical Journal*, *12*(2), 59–81.

Fanget, A. S., Berné, S., Jouet, G., Bassetti, M. A., Dennielou, B., Maillet, G. M., & Tondut, M. (2014). Impact of relative sea level and rapid climate changes on the architecture and lithofacies of the Holocene Rhone subaqueous delta (Western Mediterranean Sea). *Sedimentary Geology*, *305*, 35–53. https://doi.org/10.1016/j.sedgeo.2014.02.004

Fielding, C. R., Trueman, J. D., & Alexander, J. (2005a). Sharp-based, flood-dominated mouth bar sands from the Burdekin river delta of northeastern Australia: Extending the spectrum of mouth-bar facies, geometry, and stacking patterns. *Journal of Sedimentary Research*, *75*(1), 55–66. https://doi.org/10.2110/jsr.2005.006

Fielding, C. R., Trueman, J., & Alexander, J. (2005b). Sedimentology of the modern and Holocene Burdekin River Delta of north Queensland, Australia–controlled by river output, not by waves and tides. In L. Giosan & J. Bhattacharya (Eds.), *River deltas: Concepts, models and examples* (Vol. 83, pp. 467–496). SEPM, Special Publication.

Fielding, C. R., Trueman, J. D., & Alexander, J. (2006). Holocene depositional history of the Burdekin river delta of northeastern Australia: A model for a low-accommodation, highstand delta. *Journal of Sedimentary Research*, *76*(3), 411–428. https://doi.org/10.2110/jsr.2006.032

Funabiki, A., Saito, Y., Phai, V. V., Nguyen, H., & Haruyama, S. (2012). Natural levees and human settlement in the Song hong (red river) delta, northern Vietnam. *The Holocene*, *22*(6), 637–648. https://doi.org/10.1177/0959683611430847

Gaki-Papanastassiou, K., Karymbalis, E., & Maroukian, H. (2010). Recent geomorphic changes and anthropogenic activities in the deltaic plain of Pinios River in central Greece. *Bulletin of the Geological Society of Greece*, *43*(1), 409–417.

Gaki-Papanastassiou, K., Cundy, A. B., & Maroukian, H. (2011). Fluvial versus tectonic controls on the late Holocene geomorphic and sedimentary evolution of a small Mediterranean fan delta system. *The Journal of Geology*, *119*(2), 221–234. https://doi.org/10.1086/658144

Gàmez Torrent, D. (2007). *Sequence stratigraphy as a tool for water resources management in alluvial coastal aquifers: Application to the Llobregat delta (Barcelona, Spain)* Doctoral dissertation. Universitat Politècnica de Catalunya.

Ganti, V., Chu, Z., Lamb, M. P., Nittrouer, J. A., & Parker, G. (2014). Testing morphodynamic controls on the location and frequency of river avulsions on fans versus deltas: Huanghe (Yellow River), China. *Geophysical Research Letters*, *41*(22), 7882–7890. https://doi.org/10.1002/2014gl061918

Ghilardi, M. (2007). *Dynamiques spatiales et reconstitutions paléogéographiques de la plaine de Thessalonique (Grèce) à l'Holocène recent*. Doctoral dissertation, Université Paris XII Val de Marne.

Ghilardi, M., Kunesch, S., Styllas, M., & Fouache, E. (2008). Reconstruction of Mid-Holocene sedimentary environments in the central part of the Thessaloniki Plain (Greece), based on microfaunal identification, magnetic susceptibility and grain-size analyses. *Geomorphology*, *97*(3–4), 617–630. https://doi.org/10.1016/j.geomorph.2007.09.007

Giosan, L., Naing, T., Min Tun, M., Clift, P. D., Filip, F., Constantinescu, S., et al. (2018). On the Holocene evolution of the Ayeyawady megadelta. *Earth Surface Dynamics*, *6*(2), 451–466. https://doi.org/10.5194/esurf-6-451-2018

Grenfell, S. E., Ellery, W. N., & Grenfell, M. C. (2009). Geomorphology and dynamics of the Mfolozi river floodplain, KwaZulu-Natal, South Africa. *Geomorphology*, *107*(3–4), 226–240. https://doi.org/10.1016/j.geomorph.2008.12.011

Haghani, S., & Leroy, S. A. (2020). Recent avulsion history of Sefidrud, south west of the Caspian Sea. *Quaternary International*, *540*, 97–110. https://doi.org/10.1016/j.quaint.2018.06.034

He, L., Amorosi, A., Ye, S., Xue, C., Yang, S., & Laws, E. A. (2020). River avulsions and sedimentary evolution of the Luanhe fan-delta system (North China) since the late Pleistocene. *Marine Geology*, *425*, 106194. https://doi.org/10.1016/j.margeo.2020.106194

Heyvaert, V. M. A., & Walstra, J. (2016). The role of long-term human impact on avulsion and fan development. *Earth Surface Processes and Landforms*, *41*(14), 2137–2152. https://doi.org/10.1002/esp.4011

Heyvaert, V. M. A., Walstra, J., Verkinderen, P., Weerts, H. J., & Ooghe, B. (2012). The role of human interference on the channel shifting of the Karkheh River in the Lower Khuzestan plain (Mesopotamia, SW Iran). *Quaternary International*, *251*, 52–63. https://doi.org/10.1016/j.quaint.2011.07.018

Holmes, D. A. (1968). The recent history of the Indus. *The Geographical Journal*, *134*(3), 367–382. https://doi.org/10.2307/1792965

Hussein, M. A. (2011). *Morphotectonic of Shat Al-Arab River, South of Iraq* MSc thesis. University of Baghdad.

Jones, B. G., Woodroffe, C. D., & Martin, G. R. (2003). Deltas in the gulf of Carpentaria, Australia: Forms, processes, and products. In F. H. Sidi, D. Nummedal, P. Imbert, H. Darman, & H. W. Posamentier (Eds.), *Tropical deltas of Southeast Asia—Sedimentology, stratigraphy, and petroleum geology* (Vol. 76, pp. 21–43). SEPM Special Publication.

Karymbalis, E., Gaki-Papanastassiou, K., & Maroukian, H. (2007). Recent geomorphic evolution of the fan delta of the Mornos river, Greece: Natural processes and human impacts. *Bulletin of the Geological Society of Greece*, *40*(4), 1538–1551. https://doi.org/10.12681/bgsg.17057

Karymbalis, E., Gaki-Papanastassiou, K., Tsanakas, K., & Ferentinou, M. (2016). Geomorphology of the Pinios river delta, central Greece. *Journal of Maps*, *12*(sup1), 12–21. https://doi.org/10.1080/17445647.2016.1153356

Karymbalis, E., Valkanou, K., Tsodoulos, I., Iliopoulos, G., Tsanakas, K., Batzakis, V., et al. (2018). Geomorphic evolution of the Lilas river fan delta (central Evia Island, Greece). *Geosciences*, *8*(10), 361. https://doi.org/10.3390/geosciences8100361

Kazancı, N., & Gulbabazadeh, T. (2013). Sefidrud delta and quaternary evolution of the southern Caspian lowland, Iran. *Marine and Petroleum Geology*, *44*, 120–139. https://doi.org/10.1016/j.marpetgeo.2013.03.006

Kazancı, N., Gulbabazadeh, T., Leroy, S. A., & Ileri, Ö. (2004). Sedimentary and environmental characteristics of the Gilan–Mazenderan plain, northern Iran: Influence of long-and short-term Caspian water level fluctuations on geomorphology. *Journal of Marine Systems*, *46*(1–4), 145–168. https://doi.org/10.1016/j.jmarsys.2003.12.002

Kontopoulos, N., & Avramidis, P. (2003). A late Holocene record of environmental changes from the Aliki lagoon, Egion, North Peloponnesus, Greece. *Quaternary International*, *111*(1), 75–90. https://doi.org/10.1016/s1040-6182(03)00016-8

Koutsios, A., Kontopoulos, N., Kalisperi, D., Soupios, P., & Avramidis, P. (2010). Sedimentological and geophysical observations in the delta plain of Selinous river, ancient Helike, Northern Peloponnesus Greece. *Bulletin of the Geological Society of Greece*, *43*(2), 654–662. https://doi.org/10.12681/bgsg.11228

Kravtsova, V. I., Mikhailov, V. N., & Kidyaeva, V. M. (2009). Hydrological regime, morphological features and natural territorial complexes of the Irrawaddy River Delta (Myanmar). *Water Resources*, *36*(3), 243–260. https://doi.org/10.1134/s0097807809030014

Mackey, S. D., & Bridge, J. S. (1995). Three-dimensional model of alluvial stratigraphy; theory and applications. *Journal of Sedimentary Research*, *65*(1b), 7–31. https://doi.org/10.1306/d42681d5-2b26-11d7-8648000102c1865d

Maejima, W., & Mahalik, N. K. (2002). Control of prevalent wind on the development of distributary channel systems of Mahanadi delta, India. *Journal of the Sedimentological Society of Japan*, *55*, 1–8. https://doi.org/10.4096/jssj1995.55.1

Mahalik, N. K., Das, C., & Maejima, W. (1996). Geomorphology and evolution of the Mahanadi delta, India. *Journal of Geosciences Osaka City University*, *39*, 111–122.

Maroukian, H., & Karymbalis, E. (2004). Geomorphic evolution of the fan delta of the Evinos river in western Greece and human impacts in the last 150 years. *Zeitschrift für Geomorphologie*, *48*(2), 201–217. https://doi.org/10.1127/zfg/48/2004/201

Martin, L., Suguio, K., & Flexor, J. M. (1993). As flutuações de nível do mar durante o quaternário superior e a evolução geológica de "deltas" brasileiros. *Boletim IG-USP: Publicacao Especial*, *15*, 1–186. https://doi.org/10.11606/issn.2317-8078.v0i15p01-186

Mateo, Z. R. P., & Siringan, F. P. (2007). Tectonic control of high-frequency Holocene delta switching and fluvial migration in Lingayen Gulf bayhead, northwestern Philippines. *Journal of Coastal Research*, *23*(1), 182–194. https://doi.org/10.2112/04-0152.1

Mathers, S., & Zalasiewicz, J. (1999). Holocene sedimentary architecture of the red river delta, Vietnam. *Journal of Coastal Research*, 314–325.

McGowen, J. H., Proctor, C. V., Brown, L. F., Jr., Evans, T. J., Fisher, W. L., & Groat, C. G. (1976). *Environmental geologic atlas of the Texas coastal zone–Port Lavaca area: The University of Texas at Austin* (p. 107). Bureau of Economic Geology.

Mikhailov, V. N., Kravtsova, V. I., & Magritskii, D. V. (2004). Specific features of development of the modern Sulak river delta. *Water Resources*, *31*(2), 117–132. https://doi.org/10.1023/b:ware.0000021573.53909.d7

Mikhailov, V. N., Magritsky, D. V., Kravtsova, V. I., Mikhailova, M. V., & Isupova, M. V. (2012). The response of river mouths to large-scale variations in sea level and river runoff: Case study of rivers flowing into the Caspian Sea. *Water Resources*, *39*(1), 11–43. https://doi.org/10.1134/s0097807812010083

Moodie, A. J., Nittrouer, J. A., Ma, H., Carlson, B. N., Chadwick, A. J., Lamb, M. P., & Parker, G. (2019). Modeling deltaic lobe-building cycles and channel avulsions for the Yellow River delta, China. *Journal of Geophysical Research: Earth Surface*, *124*(11), 2438–2462. https://doi.org/10.1029/2019jf005220

Morozova, G. S., & Smith, N. D. (1999). Holocene avulsion history of the lower Saskatchewan fluvial System, Cumberland Marshes, Saskatchewan–Manitoba, Canada. In N. D. Smith & J. Rogers (Eds.), *Fluvial Sedimentology VI* (pp. 231–249). Wiley & Sons.

Morozova, G. S., & Smith, N. D. (2000). Holocene avulsion styles and sedimentation patterns of the Saskatchewan river, Cumberland Marshes, Canada. *Sedimentary Geology*, *130*(1–2), 81–105. https://doi.org/10.1016/s0037-0738(99)00106-2

Mulrennan, M. E., & Woodroffe, C. D. (1998). Holocene development of the lower Mary River plains, Northern Territory, Australia. *The Holocene*, *8*(5), 565–579. https://doi.org/10.1191/095968398676885724

Muñoz-Salinas, E., Castillo, M., Sanderson, D., & Kinnaird, T. (2017). Geochronology and landscape evolution of the strand-plain of the Usumacinta and Grijalva rivers, southern Mexico. *Journal of South American Earth Sciences*, *79*, 394–400. https://doi.org/10.1016/j.jsames.2017.08.021

Nageswara Rao, K., Saito, Y., Kumar, K. C. V. N., Kubo, S., Pandey, S., Li, Z., et al. (2020). Holocene evolution and Anthropocene destruction of the Krishna delta on the east coast of India: Delta lobe shifts, human impacts, and sea-level history. *Marine Geology*, *427*, 106229. https://doi.org/10.1016/j.margeo.2020.106229

Nageswara Rao, K., Saito, Y., Nagakumar, K. C. V., Demudu, G., Rajawat, A. S., Kubo, S., & Li, Z. (2015). Palaeogeography and evolution of the Godavari delta, east coast of India during the Holocene: An example of wave-dominated and fan-delta settings. *Palaeogeography, Palaeoclimatology, Palaeoecology*, *440*, 213–233. https://doi.org/10.1016/j.palaeo.2015.09.006

Nanson, G. C., Price, D. M., Short, S. A., Young, R. W., & Jones, B. G. (1991). Comparative uranium-thorium and thermoluminescence dating of weathered quaternary alluvium in the tropics of northern Australia. *Quaternary Research*, *35*(3-Part1), 347–366. https://doi.org/10.1016/0033-5894(91)90050-f

Nijhuis, A. G. (2013). *Fluvio-deltaic response to relative sea-level fall: A case study of the Goose River delta, Labrador, Canada* MSc thesis. Boston College.

Nooren, K. (2017). *Holocene evolution of the Tabasco delta–Mexico: Impact of climate, volcanism and humans* (Vol. 144). Utrecht Studies in Earth Sciences, Utrecht University.

Parcharidis, I., Kourkouli, P., Karymbalis, E., Foumelis, M., & Karathanassi, V. (2013). Time series synthetic aperture radar interferometry for ground deformation monitoring over a small scale tectonically active deltaic environment (Mornos, Central Greece). *Journal of Coastal Research*, *29*(2), 325–338.

Phillips, J. D. (2012). Log-jams and avulsions in the San Antonio river delta, Texas. *Earth Surface Processes and Landforms*, *37*(9), 936–950. https://doi.org/10.1002/esp.3209

Piper, D. J. W., & Panagos, A. G. (1981). Growth patterns of the Acheloos and Evinos deltas, western Greece. *Sedimentary Geology*, *28*(2), 111–132. https://doi.org/10.1016/0037-0738(81)90060-9

Provansal, M., Pichard, G., & Anthony, E. J. (2015). Geomorphic changes in the Rhône delta during the LIA: Input from the analysis of ancient maps. In M. Maanan & M. Robin (Eds.), *Sediment fluxes in coastal areas* (pp. 47–72). Springer.

Ramasamy, S. M., Bakliwal, P. C., & Verma, R. P. (1991). Remote sensing and river migration in Western India. *International Journal of Remote Sensing*, *12*(12), 2597–2609. https://doi.org/10.1080/01431169108955288

Ramasamy, S. M., Saravanavel, J., Yadava, M. G., & Ramesh, R. (2006). Radiocarbon dating of some palaeochannels in Tamil Nadu and their significance. *Current Science*, *91*(12), 1609–1613.

Resmi, M. R., Achyuthan, H., & Jaiswal, M. K. (2017). Middle to late Holocene paleochannels and migration of the Palar river, Tamil Nadu: Implications of neotectonic activity. *Quaternary International*, *443*, 211–222. https://doi.org/10.1016/j.quaint.2016.05.002

Rey, T., Lefevre, D., & Vella, C. (2009). Deltaic plain development and environmental changes in the Petite Camargue, Rhone Delta, France, in the past 2000 years. *Quaternary Research*, *71*(3), 284–294. https://doi.org/10.1016/j.yqres.2008.10.007

Roberts, H. H. (1997). Dynamic changes of the Holocene Mississippi river delta plain: The delta cycle. *Journal of Coastal Research*, *13*(3), 605–627.

Rossetti, D. F., Polizel, S. P., Cohen, M. C. L., & Pessenda, L. C. R. (2015). Late Pleistocene–Holocene evolution of the Doce River delta, southeastern Brazil: Implications for the understanding of wave-influenced deltas. *Marine Geology*, *367*, 171–190. https://doi.org/10.1016/j.margeo.2015.05.012

Ruiz-Pérez, J. M., & Carmona, P. (2019). Turia river delta and coastal barrier-lagoon of Valencia (Mediterranean coast of Spain): Geomorphological processes and global climate fluctuations since Iberian-Roman times. *Quaternary Science Reviews*, *219*, 84–101. https://doi.org/10.1016/j.quascirev.2019.07.005

Rutishauser, S., Erasmi, S., Rosenbauer, R., & Buchbach, R. (2017). SARchaeology—Detecting palaeochannels based on high resolution radar data and their impact of changes in the settlement pattern in Cilicia (Turkey). *Geosciences*, *7*(4), 109. https://doi.org/10.3390/geosciences7040109

Sarker, M. H., Akter, J., & Rahman, M. M. (2013). Century-scale dynamics of the Bengal Delta and future development. In *Proceedings of the 4th international conference on water and flood management* (pp. 91–104).

Serrano Suarez, B. E. (2004). The Sinú river delta on the northwestern Caribbean coast of Colombia: Bay infilling associated with delta development. *Journal of South American Earth Sciences*, *16*(7), 623–631. https://doi.org/10.1016/j.jsames.2003.10.005

Singh, P., Yadava, M. G., Ahmad, M. Z., Mohapatra, P. P., Laskar, A. H., Doradla, S., et al. (2015). Fertile farmlands in Cauvery delta: Evolution through LGM. *Current Science*, 218–225.

Somoza, L., Barnolas, A., Arasa, A., Maestro, A., Rees, J. G., & Hernández-Molina, F. J. (1998). Architectural stacking patterns of the Ebro delta controlled by Holocene high-frequency eustatic fluctuations, delta-lobe switching and subsidence processes. *Sedimentary Geology*, *117*(1–2), 11–32. https://doi.org/10.1016/s0037-0738(97)00121-8

Somoza, L., & Rodríguez-Santalla, I. (2014). Geology and geomorphological evolution of the Ebro river delta. In F. Gutiérrez & M. Gutiérrez (Eds.), *Landscapes and landforms of Spain* (pp. 213–227). Springer.

Stanley, D. J., & Warne, A. G. (1993). Nile delta: Recent geological evolution and human impact. *Science*, *260*(5108), 628–634. https://doi.org/10.1126/science.260.5108.628

Stanley, J. D., Warne, A. G., & Schnepp, G. (2004). Geoarchaeological interpretation of the Canopic, largest of the relict Nile Delta distributaries, Egypt. *Journal of Coastal Research*, *20*(3), 920–930. https://doi.org/10.2112/1551-5036(2004)20[920:giotcl]2.0.co;2

Styllas, M. (2018). Natural processes versus human impacts during the last century: A case study of the Aliakmon river delta. In N. Skoulikidis, E. Dimitriou, & I. Karaouzas (Eds.), *The rivers of Greece* (pp. 31–49). Springer.

Syvitski, J. P., Kettner, A. J., Overeem, I., Giosan, L., Brakenridge, G. R., Hannon, M., & Bilham, R. (2013). Anthropocene metamorphosis of the Indus Delta and lower floodplain. *Anthropocene*, *3*, 24–35. https://doi.org/10.1016/j.ancene.2014.02.003

Tanabe, S., Saito, Y., Vu, Q. L., Hanebuth, T. J., Ngo, Q. L., & Kitamura, A. (2006). Holocene evolution of the Song Hong (Red River) delta system, northern Vietnam. *Sedimentary Geology*, *187*(1–2), 29–61. https://doi.org/10.1016/j.sedgeo.2005.12.004

Törnqvist, T. E., Kidder, T. R., Autin, W. J., van der Borg, K., de Jong, A. F., Klerks, C. J., et al. (1996). A revised chronology for Mississippi River subdeltas. *Science*, *273*(5282), 1693–1696. https://doi.org/10.1126/science.273.5282.1693

Van Andel, T. H. (1967). The Orinoco delta. *Journal of Sedimentary Research*, *37*(2), 297–310.

van Gelder, A., van den Berg, J. H., Cheng, G., & Xue, C. (1994). Overbank and channelfill deposits of the modern Yellow River delta. *Sedimentary Geology*, *90*(3–4), 293–305. https://doi.org/10.1016/0037-0738(94)90044-2

Vespremeanu-Stroe, A., Preoteasa, L., Zăinescu, F., & Tătui, F. (2017a). The evolution of Danube delta after Black Sea reconnection to World Ocean. In M. Radoane & A. Vespremeanu-Stroe (Eds.), *Landform dynamics and evolution in Romania* (pp. 521–549). Springer.

Vespremeanu-Stroe, A., Zăinescu, F., Preoteasa, L., Tătui, F., Rotaru, S., Morhange, C., et al. (2017b). Holocene evolution of the Danube delta: An integral reconstruction and a revised chronology. *Marine Geology*, *388*, 38–61. https://doi.org/10.1016/j.margeo.2017.04.002

von Nagy, C. (2011). Coastal deltaic dynamics, human settlement, and ancient Olmec polities in Tabasco, Mexico. In *76th annual meeting of the Society for American Archaeology, Sacramento, California, April 1, 2011*.

Vött, A., Schriever, A., Handl, M., & Brückner, H. (2007a). Holocene palaeogeographies of the central Acheloos River delta (NW Greece) in the vicinity of the ancient seaport Oiniadai. *Geodinamica Acta*, *20*(4), 241–256. https://doi.org/10.3166/ga.20.241-256

Vött, A., Schriever, A., Handl, M., & Brückner, H. (2007b). Holocene palaeogeographies of the eastern Acheloos river delta and the lagoon of Etoliko (NW Greece). *Journal of Coastal Research*, *23*(4), 1042–1066. https://doi.org/10.2112/06-0716.1

Wang, Y., Ren, M. E., & Zhu, D. (1986). Sediment supply to the continental shelf by the major rivers of China. *Journal of the Geological Society*, *143*(6), 935–944. https://doi.org/10.1144/gsjgs.143.6.0935

Weinstein, R. A., & Junkin, G. M. (1992). Natural setting. In R. A. Weinstein (Ed.), *Archaeology and paleogeography of the lower Guadalupe River/San Antonio bay region: Cultural Resources investigations along the channel to Victoria, calhoun and Victoria counties, Texas, 7–22*. Coastal Environments, Inc.

Welder, F. A. (1955). *Deltaic processes in Cubits Gap Area, Plaquemines Parish, Louisiana* Doctoral dissertation. Louisiana State University and Agricultural & Mechanical College.

Woodroffe, C. D., & Chappell, J. (1993). Holocene emergence and evolution of the McArthur river delta, southwestern gulf of Carpentaria, Australia. *Sedimentary Geology*, *83*(3–4), 303–317. https://doi.org/10.1016/0037-0738(93)90018-z

Wang, Y., Liu, X., Li, G., & Zhang, W. (2016). Stratigraphic variations in the Diaokou lobe area of the Yellow river delta, China: Implications for an evolutionary model of a delta lobe. In P. D. Clift, J. Harff, J. Wu, & Y. Qui (Eds.), *River-dominated shelf sediments of East Asian seas* (Vol. 429, pp. 185–195). Geological Society, London, Special Publications.

Zheng, S., Wu, B., Wang, K., Tan, G., Han, S., & Thorne, C. R. (2017). Evolution of the Yellow River delta, China: Impacts of channel avulsion and progradation. *International Journal of Sediment Research*, *32*(1), 34–44. https://doi.org/10.1016/j.ijsrc.2016.10.001